NOVEL FABRICATION OF CELLULOSE NITRATE NANOFIBER MATS

A Thesis

Presented to the Faculty of the Graduate School

of Cornell University

In Partial Fulfillment of the Requirements for the Degree of

Master of Science in Fiber Science

by

Katherine Michelle Hammes

January 2012

ABSTRACT

Cellulose derivatives were electrospun into nonwoven nanofiber mats via two fabrication routes, both of which produced appropriate physical and chemical properties to support biological indicators: (1) spinning of cellulose nitrate directly and (2) nitration of cellulose acetate nonwoven mats after spinning. For both methods, the morphology of the fibers was analyzed through scanning electron microscopy (SEM) and use of ImageJ software; the chemical structure of the polymer was analyzed through Fourir transform infrared spectroscopy (FTIR) and X-ray photoelectron spectroscopy (XPS); and tensile strength of each nonwoven mat was analyzed through tensile testing. Ultimately, both approaches produced nanofiber mats with comparable physical properties. However, only the mats from the first method contained nitrate groups at the fiber surface.

BIOGRAPHICAL SKETCH

Katherine Hammes grew up in Leawood, Kansas. There, she attended Shawnee Mission East High School where she completed the International Baccalaureate Program in 2005. For college, she attended Illinois Institute of Technology where she graduated with Honors in Chemical Engineering in 2009. After finishing her Masters of Science in Fiber Science at Cornell University, she went on to work for the Skincare Global Research Center for Unilever in Trumbull, Connecticut. She currently resides in New Haven, Connecticut.

ACKNOWLEDGMENTS

I would like to thank the Frey Lab, the Fiber Science and Apparel Design Department of Cornell University, and the Cornell Center for Materials Research for making this project possible.

TABLE OF CONTENTS

LIST OF FIGURES

LIST OF TABLES

LIST OF ABBREVIATIONS

Abbreviation	*Meaning*
CA	Cellulose Acetate
cm	Centimeter(s)
CN	Cellulose Nitrate
FTIR	Fourier Transform Infrared Spectroscopy
hr	Hour
kV	Kilovolt(s)
M	Molar
min	Minute
mm	Milimeter(s)
μm, μL	Micrometer(s), Microliter(s)
MPa	Megapascal(s)
N	Newton
SEM	Scanning Electron Microscopy
v:v or v/v	Volume to Volume Ratio
wt%	Weight Percent
XPS	X-ray Photoelectron Spectroscopy

CHAPTER 1

Introduction

Background

Due to their unique properties, fibers have recently been incorporated into a variety of new materials for use in non-textile applications—ranging from super-strong carbon fiber composites to highly efficient fiber-optic cables [**1**]-[**2**]. One such emerging application is the use of nanofiberous membranes in biomedical and biological engineering [**3**]-[**6**]. These materials easily lend themselves as an appropriate medium for cell growth, catalysts, indicators, or biosensors due to their unique shape: because nanofibers possess a high surface area to volume ratio, abundant reaction or adhesion at the surface can be achieved with a relatively small amount of membrane material [**7**].

To make these nanofibrious membranes, a process is used called electrospinning. Electrospinning is a fabrication method which utilizes an electric charge gradient rather than a mechanical force to synthesize both individual fibers with diameters in the micro/nano range and also non-woven fabrics from such fibers [**8**]-[**10**]. When electrospinning from polymer solution, the spinning apparatus consists of a syringe supplying the spinning dope to a charged needle, an air gap of 5-20 centimeters, and a grounded metal collection plate. As the spinning dope is pushed through the syringe tip, the voltage difference between the syringe and the collection plate forces the polymer solution across the air gap, simultaneously allowing the solvent to evaporate and drawing the polymer (solute) into an ultra-fine fiber [**8**]. As these fibers are deposited randomly on the collection plate, they can form isotropic mats of nonwoven fabrics [**9**].

To produce biocompatible membranes through electrospinning, many materials can potentially be used. In recent years, electrospinning has been shown to

have promising results for a variety of both melt and solution spinning dopes, producing fibers containing materials ranging from polymers to ceramics and composites [**10**]. Among these materials is a water soluble B-complex vitamin called biotin, which is often used as a protein binding site for biological indicators or biosensors [**11**]-[**14**]. Previously, biotin has been incorporated into polylactic acid nanofiber mats for such use [**15**]. In this case, biotin was added to the spinning dope directly and biotin at the fiber surface successfully bound streptavidin protein; however, most of the biotin was not at the fiber surface and therefore was not available for protein binding [**16**].

To improve on these results, another option could be to spin fibers from biocompatible polymers that bind readily with proteins and would not require an additive, such as biotin, for binding to occur. One such polymer is cellulose-nitrate, an explosive derivative of cellulose which can easily bind due to its active nitrate groups and has long shown biocompatibility [**17**]-[**20**]. As a non-fibrous membrane, cellulose nitrate filters have been successfully used as a binding site for an array of biological components including fragments of DNA, RNA, nucleic acids, and proteins, showing considerably superior results when compared with similar materials [**21**]. This makes cellulose nitrate an ideal material to explore as a possible option for biocompatible nanofibrious membranes.

Previously, fibers containing cellulose and its derivatives have been produced from solution electrospinning under a multitude of spinning conditions, with particular viability shown for cellulose-acetate to produce consistent fibers and robust nonwoven mats [**22**], [**23**]. Conversely, cellulose-nitrate-acetate has only shown limited spinning success, producing fibers with inconsistent diameters and nonwoven fabrics which were flimsy and fluffy [**24**]. Building on this previous work, the production of robust cellulose nitrate nanofiber membranes could be achieved two ways. Either the surface

functionality of robust cellulose-acetate membranes could be altered to incorporate a nitrate group, or the cohesion of flimsy cellulose-nitrate membranes could be altered to improve robustness.

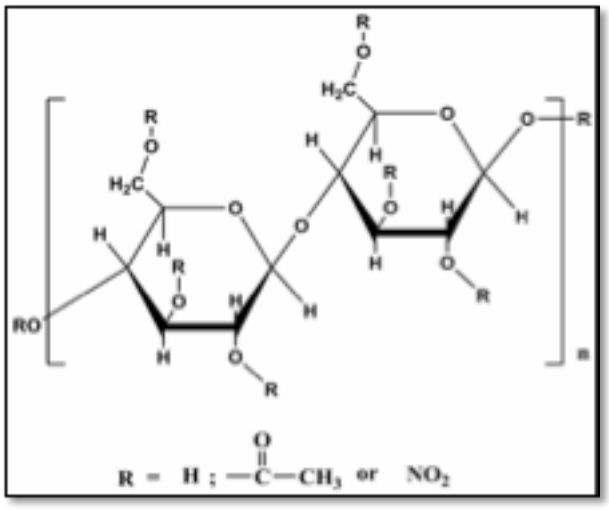

Figure 1: Cellulose-Nitrate-Acetate [24]

The manipulation of the surface functionality of nanofibers has been explored through multiple approaches, including the manipulation of the spinning dope and the use of reactive blocking treatments post-spinning [**25**], [**26**]. In the specific case of surface functionalizing cellulose, whether fibrous or otherwise, most work has centered around the idea of bulk surface treatment after fabrication [27]. These studies have produced a range of success. In one study, cyclohexane plasma was tested with the intention to functionalize the surface of cellulose filter paper through the deposition of a hydrophobic polymer layer. However, although the morphology of the filter paper was maintained, no significant change was noted in the hydrophobic adhesion at the surface [**28**]. In another study, nanofibers of bacterial cellulose were acetylated at the surface while maintaining the fiber morphology. In this case, the fibers were treated with varying amounts of acetic anhydride in a solution of acetic

acid, toluene, and perchloric acid [**29**]. In yet another work, saline surface treatment of microfillibrated cellulose within a cellulose acetate matrix has shown promising results in simultaneously increasing tensile strength and surface hydrophobicity [30]. These previous findings give a positive outlook on the possibility of surface functionalizing of cellulose acetate membranes.

In this case, the surface of the cellulose acetate nanofibers would need to be altered to include a nitrate group, thus involving nitration [**31**]. The established methods for nitrating cellulose are varied in both starting materials and nitration reagents, and none produce a complete conversation of all three functional groups to nitrate. In an early study, a 99% yield of 3,6-dinitrate was produced by the reaction of cotton with pyridine-hydroxylamine [**32**]. In yet another study, various schemes of nitration were tested using two different cellulose sources (wood powder and wood cellulose) and two different nitration reagents (a mixture of nitric acid and phosphorous pentaoxide and a mixture of nitric acid and acetic anhydride) to produce a 95% conversion to cellulose trinitrate [**33**]. Nitration can also be directly carried out using only nitric acid as a reagent [**31**], [**34**].

In addition to the surface functionality of cellulose-based nanofiber membranes, robustness and strength are also key factors in evaluating usefulness. One common model which is used to explain the tensile behavior of fibers is the random fiber bundle (RFB) model, which assumes that the strength of the fibers is distributed uniformly within a finite interval and that the global load is shared among all unbroken fibers in the bundle [**35**]-[**37**]. For electrospun fibers, it is theorized that high surface interaction also plays a role. In nanofibers, strength is expected to not only derive from the mechanical interlocking mechanism of load transfer (due to the irregular void structure of the nonwoven membrane) but also to come from increased surface adhesion (due to the high surface area of the fibers) [**38**]. Therefore, an

increase in the adhesion between individual fibers would likely increase the overall robustness of a nanofiber membrane.

Although cellulose and its derivatives have been used in a range of biocompatible materials, no unifying theory has been widely accepted to explain its adhesion phenomena. This owes largely to an overlap in mechanical, physical, and chemical forces [39]. In addition, the shape of a cellulose-based material can also impact its properties. In the case of cellulose fibers, the effect of hydrogen bonds at the surface becomes more pronounced during fiber-fiber interactions as the fiber diameter moves to the nano-scale [39]. This fiber-fiber bond could likely be further increased through treatment post-fabrication, namely from thermal or solvent bonding [**40**]. Due to the explosive nature of cellulose nitrate when heated, thermal bonding is likely to be a safer option [**31**].

Research Approach

This research project attempted to build on previous results by producing nanofiber mats with active nitrate groups at the surface and improved tensile properties. Two approaches were investigated to achieve this goal: the first approach was to spin cellulose-nitrate directly and subsequently increase the fiber bonding through finishing steps; the second approach was to spin cellulose-acetate and then perform a nitration at the surface of the spun fiber. For both methods, the morphology of the fibers was analyzed through scanning electron microscopy (SEM) and use of ImageJ software; the chemical structure of the polymer was analyzed through Fourir transform infrared spectroscopy (FTIR) and X-ray photoelectron spectroscopy (XPS); and tensile strength of each nonwoven mat was analyzed through tensile testing. SEM verified the physical structure of the sample, confirming that the mats are comprised of nanofibers, and illuminated any visual changes in the morphology of the sample

before and after treatment. This technique worked through measurement of the interactions of a beam of electrons with the surface of the sample, producing detailed images. These images were further analyzed using ImageJ software to measure changes in average pore size. FTIR was used to verify the bulk chemical structure of each sample and more specifically to determine the presence of nitrate groups within each sample. This technique worked through obtaining an infrared spectrum of absorbance or emission over a large range of wavelengths. These spectra were compared to the spectra of known materials to determine or verify chemical structure. In addition, the chemical structure at the surface was more closely examined using XPS. This technique worked through measurement of the kinetic energy and number of electrons which escape from the surface of the material while being irradiated with a beam of x-rays. Based on previously known energy states of each element, the elements and their relative concentration at the surface can be determined. Finally, tensile testing was used to determine the nature of the fiber-fiber bonding within mats after various treatments. For each tensile test, a sample was held between two clamps and pulled at a constant rate and force to determine characteristics of its tensile strength, including insights into the elasticity/brittleness of each sample and its maximum load to break. The specific objectives of this project were thus outlined.

Objectives

The goal of this project was to create robust cellulose-nitrate mats through two novel processes. To analyze and characterize these mats, the following hypotheses were tested:

Method 1: Spinning of Cellulose Nitrate Fibers Directly

Hypothesis 1.1: Cellulose-nitrate can be consistently made into uniform solutions.

Hypothesis 1.2: Cellulose-nitrate solutions can be electrospun into nanofibers, ultimately forming nonwoven mats.

Hypothesis 1.3: The mechanical properties of cellulose-nitrate mats can be changed through finishing steps designed to improve fiber-fiber bonding.

Method 2: Spinning and Subsequent Nitration of Cellulose Acetate Fibers

Hypothesis 2.1: Cellulose-acetate can be consistently made into uniform solutions.

Hypothesis 2.2: Cellulose-acetate solutions can be electrospun into nanofibers, ultimately forming nonwoven mats.

Hypothesis 2.3: The bonding and chemical structure at the surface of cellulose-acetate mats can be changed through controlled nitration, changing the tensile strength and mechanical properties of the mats.

Preliminary Work and Experimental Design

A variety of preliminary tests were used to determine a viable solvent system, ideal spinning conditions, and the most promising range of finishing treatments for the final experiments with both cellulose acetate and cellulose nitrate. In both cases, a solvent system and concentration were chosen, spinning conditions were established, and finishing treatments were tested.

Cellulose Acetate

Originally, the intention of this project was to improve the cohesion of cellulose-nitrate-acetate nanofiber mats outlined in previous work [**24**]. In this previous method, cellulose acetate was first nitrated and then spun. However, after many attempts, these results could not be replicated, because the cellulose-nitrate-acetate would not dissolve in acetone as described. In hindsight, this could possibly be due to the reaction degrading the cellulose-acetate rather than producing cellulose-nitrate-acetate. It was, nevertheless, observed that the cellulose acetate would become "sticky" or "gum-like" during the nitration process. Therefore, the idea of spinning cellulose acetate first, then nitrating the surface under mild conditions was pursued instead. This nitration, it was thought, would achieve two main goals in one step: both increasing the cohesion between the fibers as the surfaces become "sticky" and increasing the number of nitrate groups available at the surface.

Since robust and repeatable methods for the dissolving and spinning of cellulose acetate had previously been established [**41**], these solution and electrospinning conditions were adopted. To determine the range of nitration conditions that would be most viable, cellulose acetate was spun onto glass slides, nitrated under various conditions, and examined via light microscopy to see if the fiber morphology was intact. Based on this preliminary data (Table 1, Figure 2), the most

viable finishing treatment conditions were determined to be 0.9M and 1.8M nitric acid for 20 minutes and 24 hours.

Table 1: Nitration Results of Cellulose Acetate Preliminary Tests

	20 Minutes	*24 Hours*
Water Only	Morphology Intact	Morphology Intact
0.9M Nitric Acid	Morphology Intact	Morphology Intact
1.8M Nitric Acid	Morphology Intact	Morphology Intact
7.9M Nitric Acid	Sample Mostly Destroyed	Sample Completely Destroyed
15.8M Nitric Acid	Sample Completely Destroyed	Sample Completely Destroyed

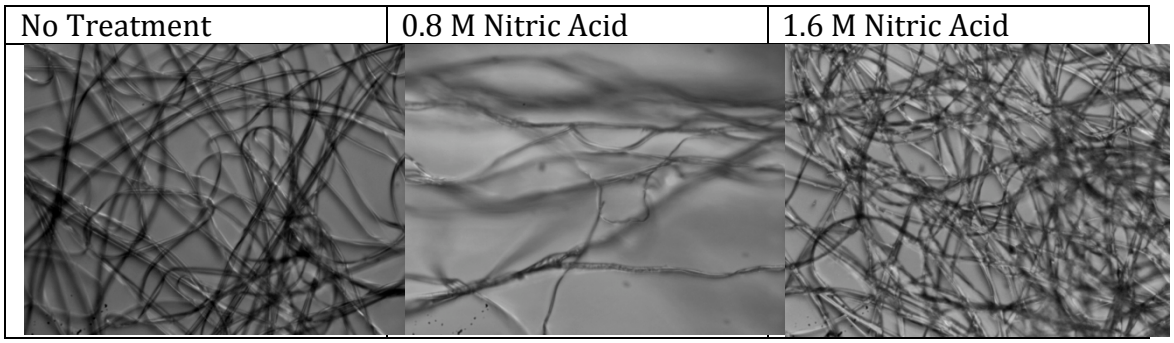

Figure 2: Cellulose acetate fibers on glass slides after 20 minutes of exposure to nitric acid.

Cellulose Nitrate

Due to its high flammability, pure cellulose nitrate is not readily available for purchase as a powdered reagent, which presented a difficulty for obtaining pre-fabricated, pure cellulose nitrate. To overcome this, filter paper made of pure cellulose nitrate was purchased instead and subsequently dissolved. After a search of available literature, no publications which involved electrospinning cellulose nitrate could be found, so a viable solvent system and spinning conditions had to be determined through systematic testing. Based on the solubility information available on cellulose nitrate [**42**], acetone and methyl-ethyl-ketone were explored as solvents (Table 2). Acetone yielded the best spinning results.

Next, treatment conditions to improve the fiber-fiber bonding of the cellulose nitrate fibers were explored. Heat treatment was ruled out due to the flammability of the cellulose nitrate. A safer alternative was explored: exposure of the samples to small concentrations of solvent. It was thought that this would allow the surface of the fibers to partially dissolve together, leaving the overall fiber morphology intact. In a preliminary test, cellulose nitrate was spun onto glass slides and exposed to various concentrations of acetone in water for either 20 minutes or 24 hours. Based on the results from this test (Table 3, Figure 3), 1:19 and 1:9 v:v Acetone:Water for 20 minutes and 24 hours were chosen as the most viable finishing treatments.

Table 2: Solubility & Spinning Results of Cellulose Nitrate Preliminary Tests

	Solution Result	*Spinning Result*
10wt% in Acetone	Clear, homogeneous solution	Fibers with some beading.
12wt% in Acetone	Clear, homogeneous solution	Uniform fibers.
12wt% in Methyl-Ethyl-Ketone	Clear, homogeneous solution	Non-uniform fibers.
14wt% in Acetone	Clear, homogeneous solution	Too viscous to spin.

Table 3: Finishing Treatment Results of Cellulose Nitrate Preliminary Tests

	20 Minutes	*24 Hours*
Water Only	Morphology Intact	Morphology Intact
1:19 v:v Acetone: Water	Morphology Intact	Morphology Intact
1:9 v:v Acetone:Water	Morphology Intact	Morphology Intact
1:1 v:v Acetone: Water	Sample Completely Destroyed	Sample Completely Destroyed
Acetone Only	Sample Completely Destroyed	Sample Completely Destroyed

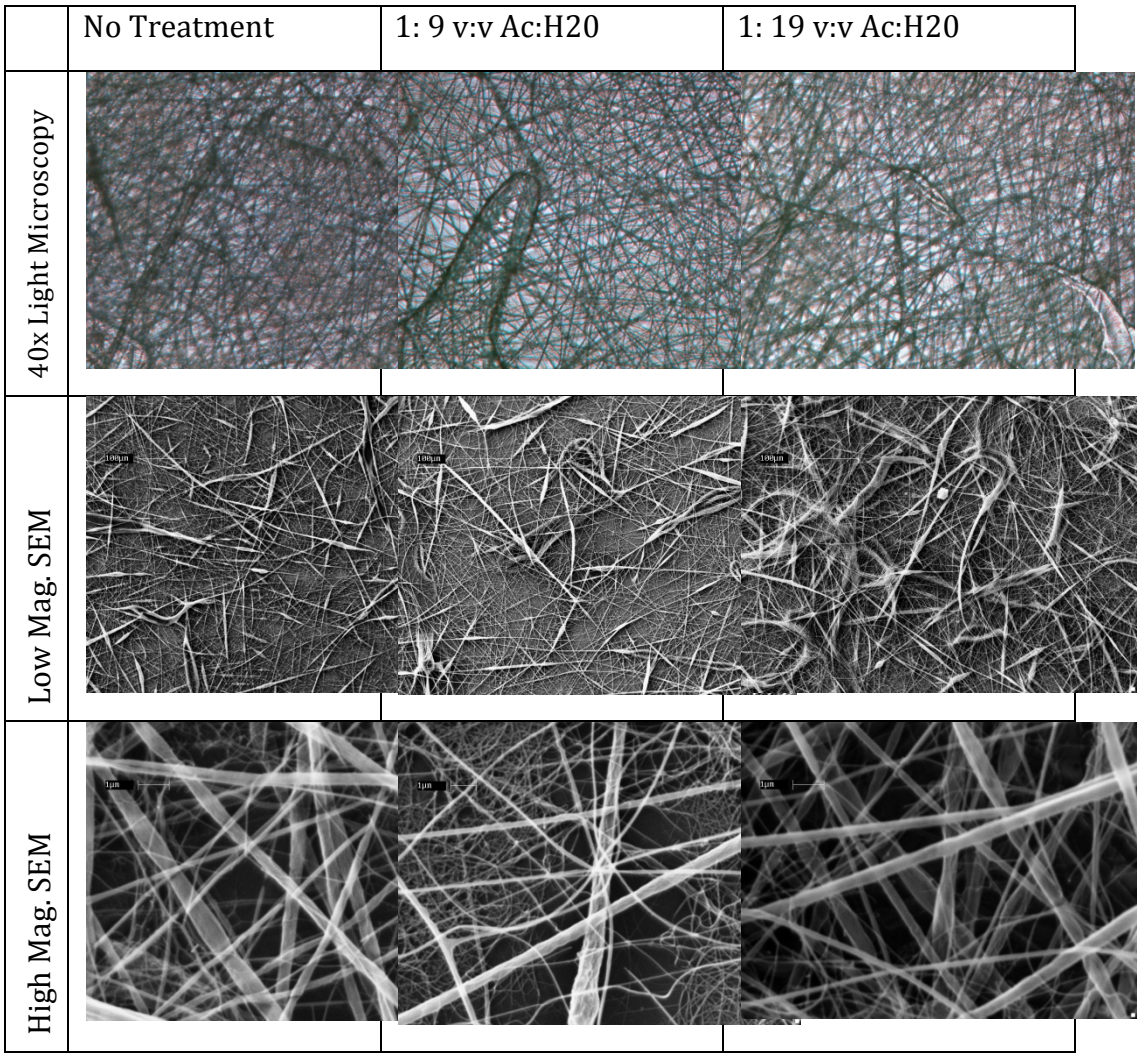

Figure 3: Cellulose nitrate on glass slides after 24 hours of treatment.

CHAPTER 2

Final Materials and Methods

Materials

Cellulose acetate (acetyl content: 39.8 wt%, Mn: 30,000) was purchased from Aldrich Chemical Co (St. Louis, MO). Whatman brand cellulose nitrate membrane filters (diameter 142mm, pore size 0.45 μm), concentrated nitric acid, and acetone were purchased from VWR International (West Chester, PA).

Preparation of Solutions

Cellulose-nitrate solutions (12 wt%) were made by dissolving cellulose-nitrate filter paper in acetone at room temperature. Cellulose-acetate solutions (17 wt%) were made by dissolving cellulose-acetate in acetone and water (85:15 Acetone: Water v/v) at room temperature. Each solution was shaken overnight using a wrist action shaker (Burrell Scientific Inc., Pittsburgh, PA) prior to spinning.

Electrospinning

The electrospinning apparatus consisted of a programmable syringe pump (Harvard Apparatus, MA) and a high-voltage supply (Gamma High Voltage Research Inc., FL). For small scale spinning, a stationary copper collection plate was used; for large scale, a rotating copper "wheel" covered in aluminum foil was used. The following conditions were used for cellulose nitrate and cellulose acetate.

Cellulose Nitrate:

Small Scale: 15 kV voltage difference, 25 μL/min flow rate, 10 cm spin distance, copper collection plate covered in aluminum foil. The preliminary samples were collected for 5 to 15 minutes.

Large Scale: 17 kV voltage difference, 15 µL/min flow rate, 6 cm spin distance, copper collection "wheel" covered in aluminum foil. The large scale sample was collected for 3 hours. This produced a nonwoven fabric 36 inches long, 6 inches of which was used for post treatment studies.

Cellulose Acetate:

Small Scale: 10 kV voltage difference, 45 µL/min flow rate, 10 cm spin distance, copper collection plate covered in aluminum foil. The preliminary samples were collected for 5 to 15 minutes.

Large Scale: 17 kV voltage difference, 20 µL/min flow rate, 6 cm spin distance, copper collection "wheel" covered in aluminum foil. The large scale sample was collected 3.5 hours. This produced a nonwoven fabric 36 inches long, 6 inches of which was used for post treatment studies.

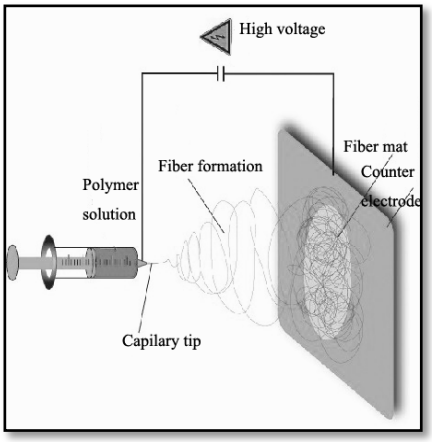

Figure 4: Electrospinning Apparatus [24]

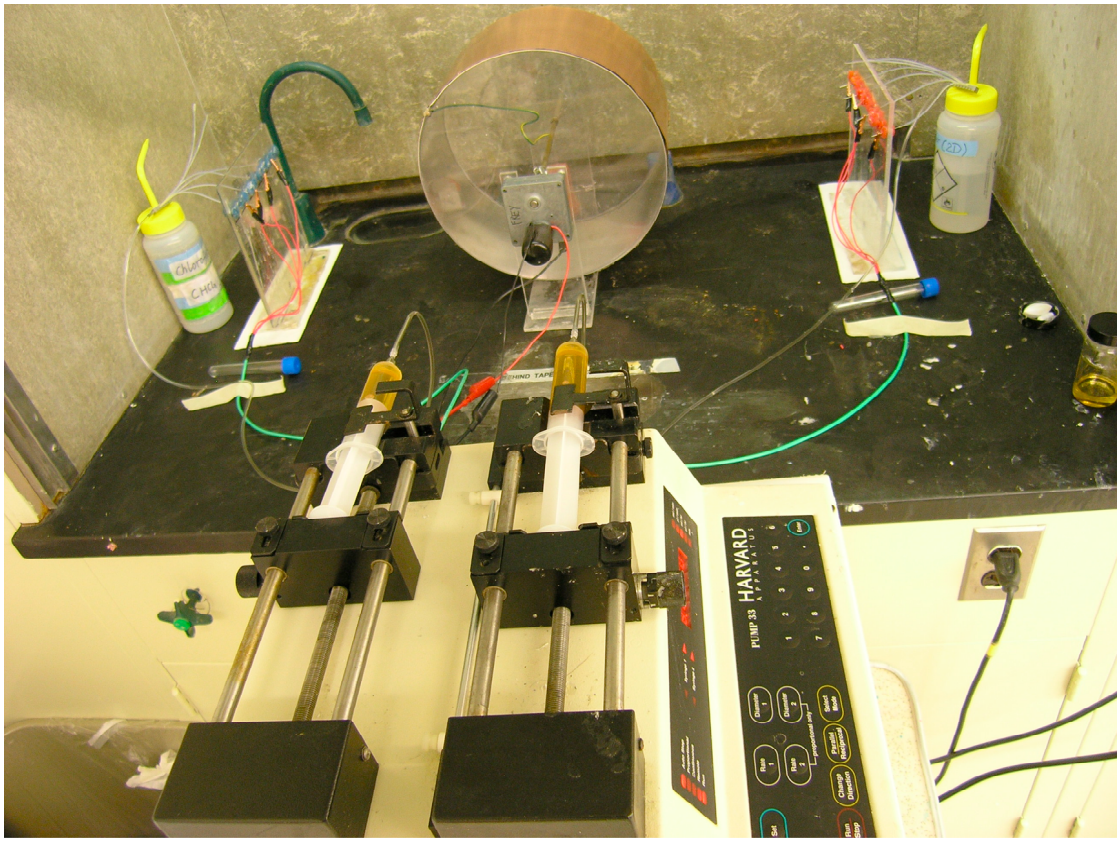

Figure 5: Copper collection "wheel" electrospinning apparatus.

Sampling

To ensure the least variation between samples, all samples for tensile tests were cut from the same piece of 6 inch by 36 inch nonwoven fabric produced from large-scale spinning. These formed approximately 6 inch square mats, which were subsequently treated and cut into smaller samples.

Finishing Treatments

The nonwoven mats were subjected to newly mixed solutions in covered pyrex Petri dishes at room temperature. In each case, a sample from large-scale spinning, which was still attached to aluminum foil, was submerged in solution for either 20 minutes or 24 hours. Each sample was subsequently dried at room temperature under vacuum for 24 hours. The nonwoven mats were subjected to varying concentrations of acetone (1:9 and 1:19 Acetone:Water v/v). The cellulose acetate nonwoven mats were subjected to varying nitric acid concentrations (1.8M and 0.9M) and were subsequently rinsed in running water for 30 minutes to remove residual acid prior to drying.

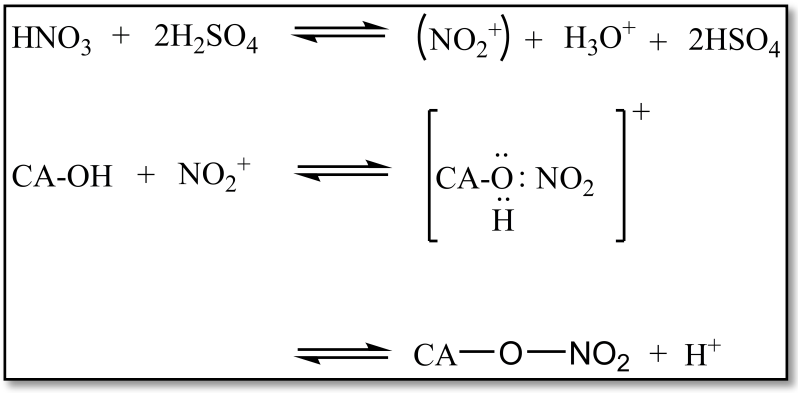

Figure 6: Synthetic Scheme of Nitration

Instron Tensile Testing

To test the mechanical properties of the fiber mats, tensile testing was performed on five samples according to ASTM standard D638-02a with an Instron 5566 equipped with a 100 N load-cell, 65% room humidity, at 23°C and crosshead speed of 10mm/min. Each sample was conditioned for at least 24 hours prior to testing. Each data point was found to be within compliance of this standard. To prepare the samples for tensile testing, each 0.02 mm thick sample

was punched into dog-bone shape with a dimension of 63.5 x 9.53 x 3.18 mm^3 (Die ASTM D-638 type V, ODC Tooling & Molds) using a manual test specimen cutting clicker press (Lucris MA Seriers 3, PAT No 666286 A).

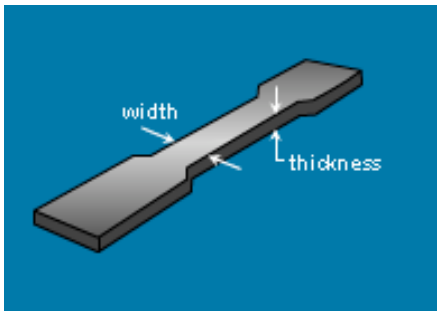

Figure 7: Schematic of Cut Tensile Sample.

Tensile data was recorded via Instron Bluehill® software (version 1.2.253) using the control mode for tensile extension and a 90% load drop. In analysis of this data, the Young's modulus was calculated by measuring the slope of the elastic region on a stress vs strain curve.

Fourier Transform Infrared Spectroscopy (FTIR)

To confirm the chemical structure of each sample, FTIR spectroscopy was performed using a PerkinElmer Nicolet Magna 560 IR spectrometer (Madison, WI). Each spectrum was collected and processed with OMNIC ® software, using 65 scans, a spectral range of 550 to 4000, a resolution of 4, a laser frequency of 15798.0 cm^{-1}, a data spacing of 1.928 cm^{-1}, an auto gain of 8, and an aperture of 69.

X-ray Photoelectron Spectroscopy (XPS)

To determine the elemental composition at the surface of each sample, XPS was performed using a Surface Science Instruments XPS model SSX-100. Each spectrum was collected under vacuum and processed with CasaXPS ® software using

10 scans, a 55 degree emission angle, a 35 degree takeoff angle, and a binding energy range between 0 and 1200 eV.

Scanning Electron Microscopy (SEM) and Image J

SEM images were produced using a Leica 440 scanning electron microscope (SEM) at 15 kV. Samples were coated for 30 seconds with 10 nm Au–Pd prior to imaging. These images were analyzed using ImageJ software to determine pore measurements.

CHAPTER 3

Results and Discussion

Following the procedures previously outlined, fifty samples each of cellulose acetate and cellulose nitrate were prepared and tested to determine their tensile properties. Five samples representing each of the eight treatments or two control conditions (no treatment) were tested based on both directions of fabrication (with or against the spin grain). This data was used to calculate the young's modulus, extension at break, and force to break for each treatment option and compare to the control (no treatment) in each case. Each data point was determined to be within compliance of the ASTM standard D638-02a, making each point accurate to a 95% confidence interval. Once broken through tensile testing, representative samples were imaged at their breakpoints via SEM and chemically characterized via FTIR and XPS.

Instron Tensile Testing

Cellulose Acetate

When examining the data for the extension at break (Figure 9) and force to break (Figure 10) of cellulose acetate, there is no statistically significant change in the elongation or strength of the mats before and after treatment. In the case of the Young's modulus (Figure 8), however, there is one treatment that produced a statistically significant loss in MPa stress per percent strain when compared to the control. This was the measurement of samples cut in the direction of the spinning grain after 24 hours of submersion in 0.9M nitric acid. Although this statistical significance is not maintained in the samples cut against the spinning grain, there does appear to be a loss in that collection of samples as well; the mean of the young's modulus for the 24 hour treatment in 0.9M nitric

acid both for and against the grain are the two lowest values among all conditions tested. This is a surprising result, because harsher treatments were also tested for longer times. One suggestion for this unexpected result is that the exposure to this low concentration of nitric acid for a longer amount of time worked to break down the chemical structure of the cellulose acetate molecules without increasing the bonding between the fibers. In other words, this treatment option may have been harsh enough to undermine the integrity of the fibers (which would make them weaker) while still being mild enough to not soften their surfaces together (which would make them stronger).

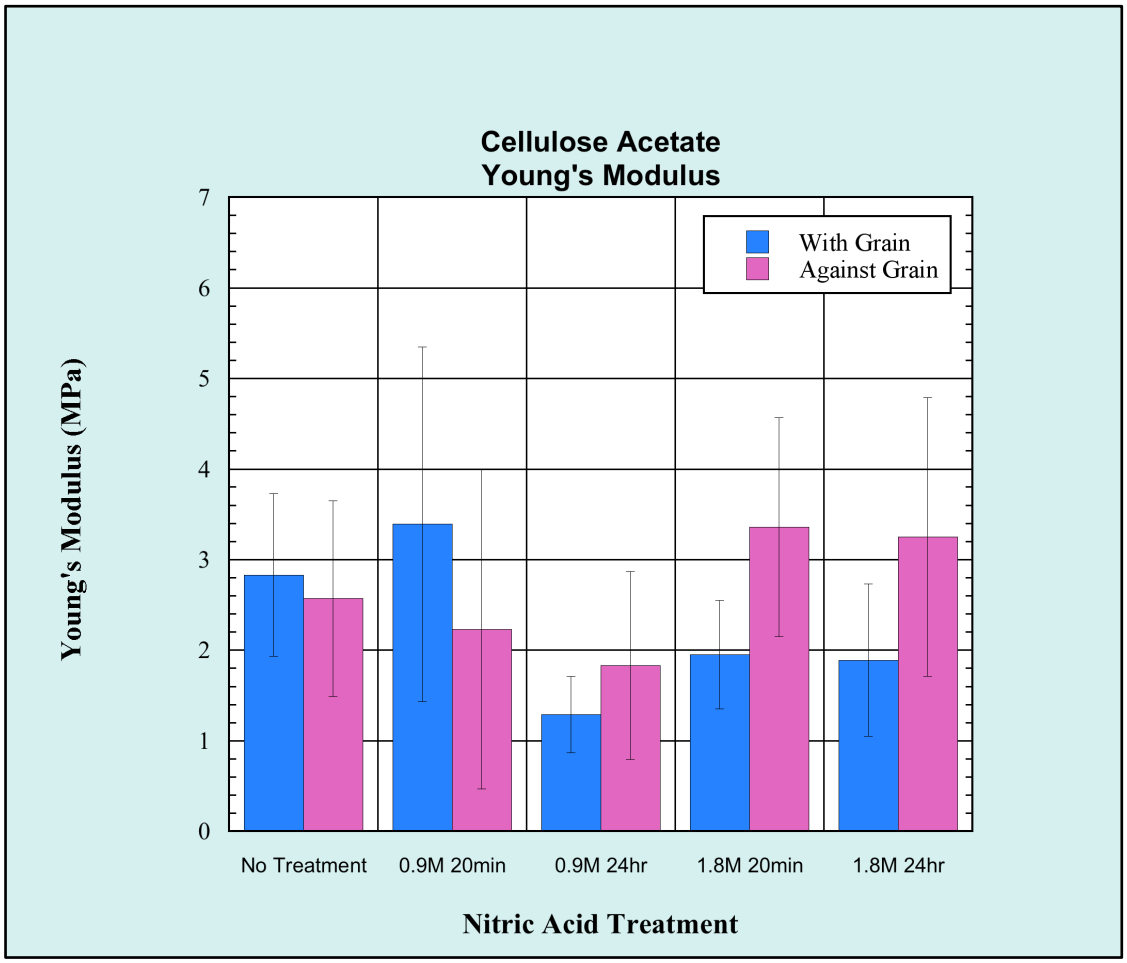

Figure 8: Young's Modulus data for cellulose acetate.

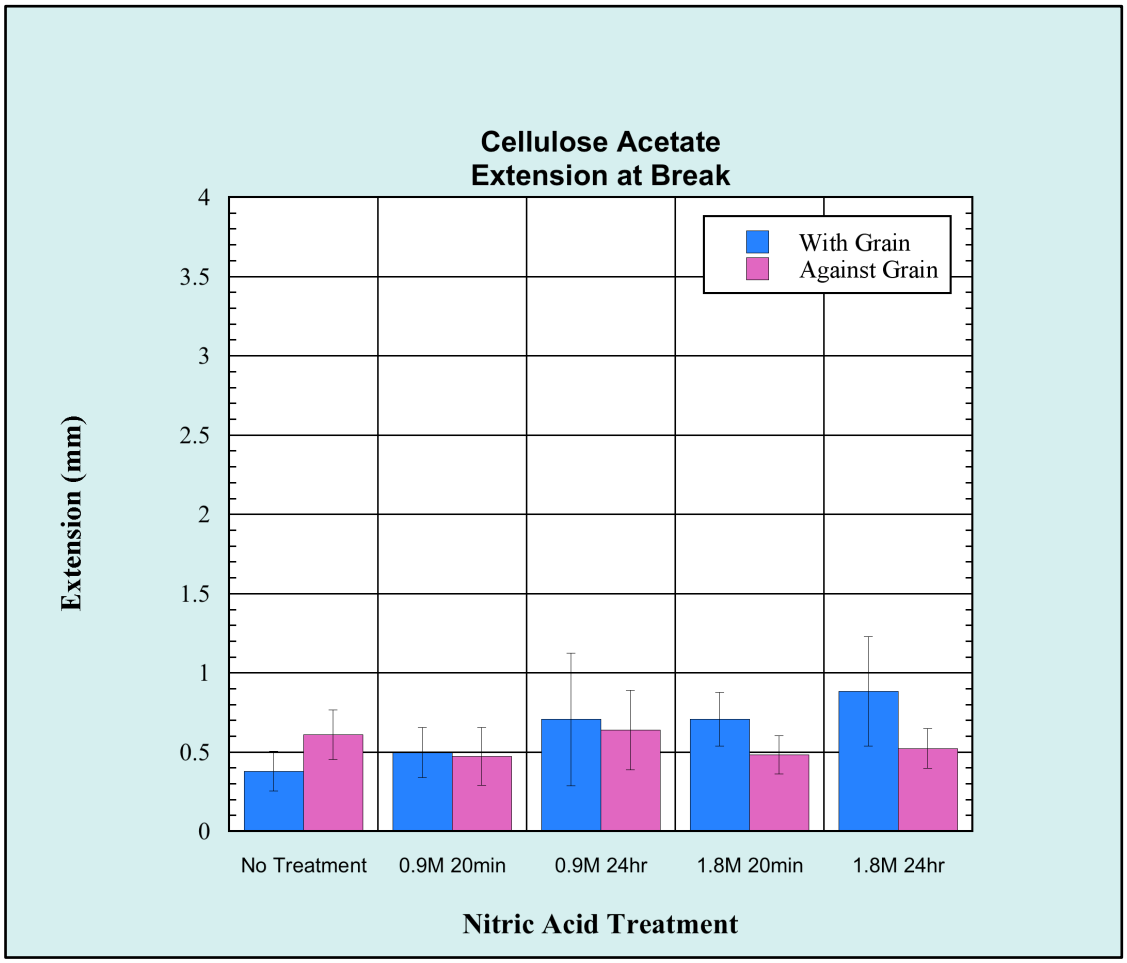

Figure 9: Extension at break data for cellulose acetate.

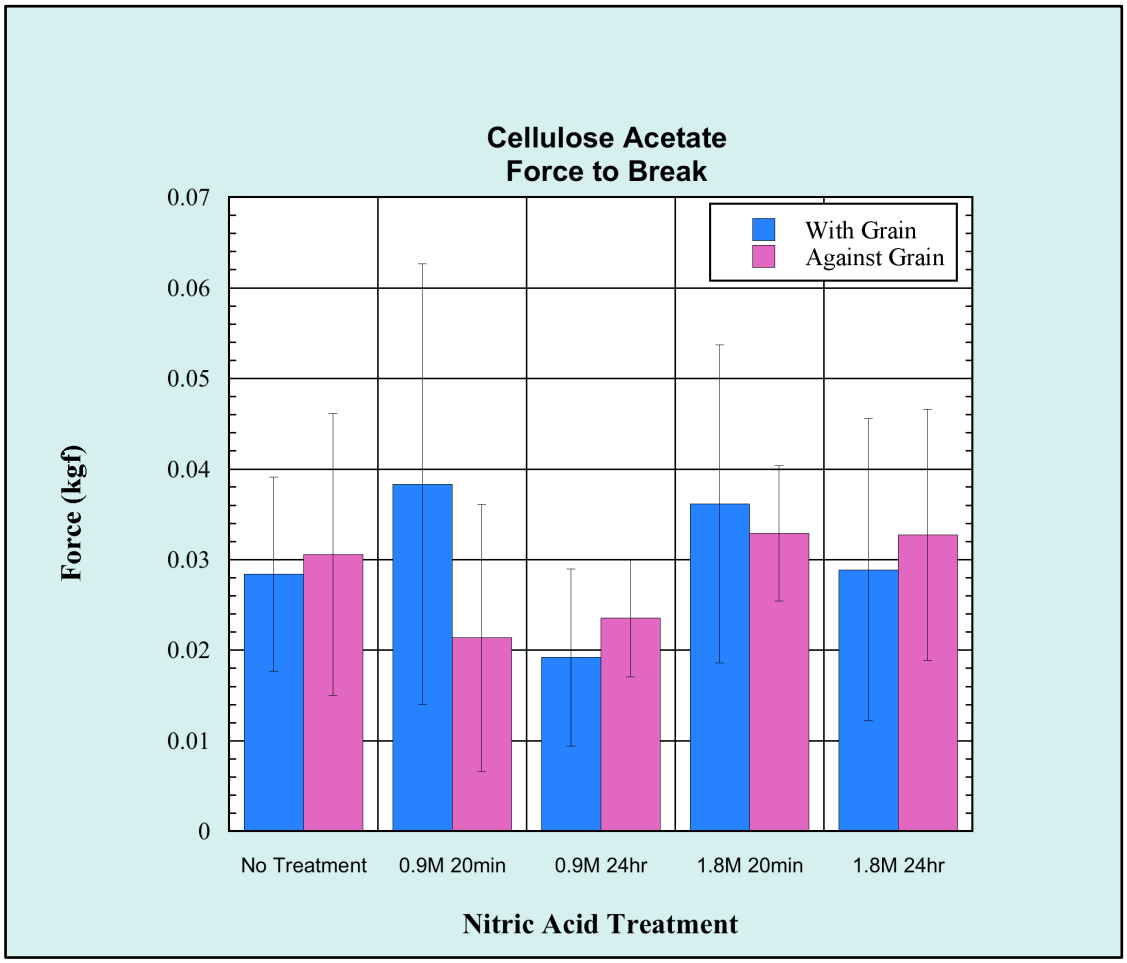

Figure 10: Force to break data for cellulose acetate.

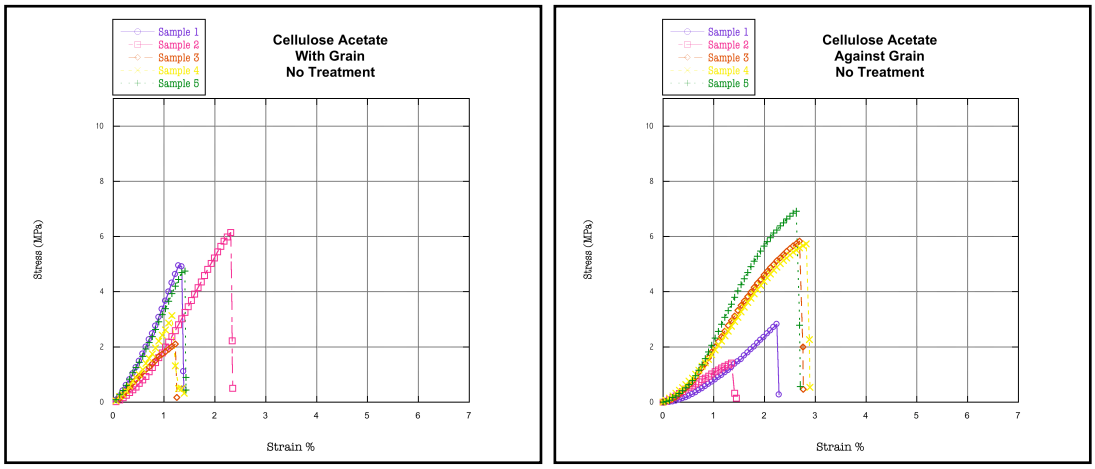

Figure 11: Graphs of tensile data of cellulose acetate before treatment with grain (a) and against grain (b).

Even without treatment, the cellulose acetate mats exhibited a sharp breakpoint suggesting that the material breaks as a continuous whole rather than falling apart slowly or breaking one fibril at a time (Figure 11). The approximately linear curves show that the breaks each occur in the elastic region of the material and that therefore the material is brittle.

When testing samples that were cut with the grain, break points were grouped closely around 1.3% strain with only one sample reaching approximately 2.4% strain before breaking, whereas samples cut against the grain exhibited the opposite strain behavior: only one sample exhibits a breakpoint at 1.4% strain while the rest are grouped between 2.2% and 2.9% strain. This suggests that the samples may be anisotropic due to the method of spinning, with samples cut with the grain breaking at a lower strain percent than those cut against the grain.

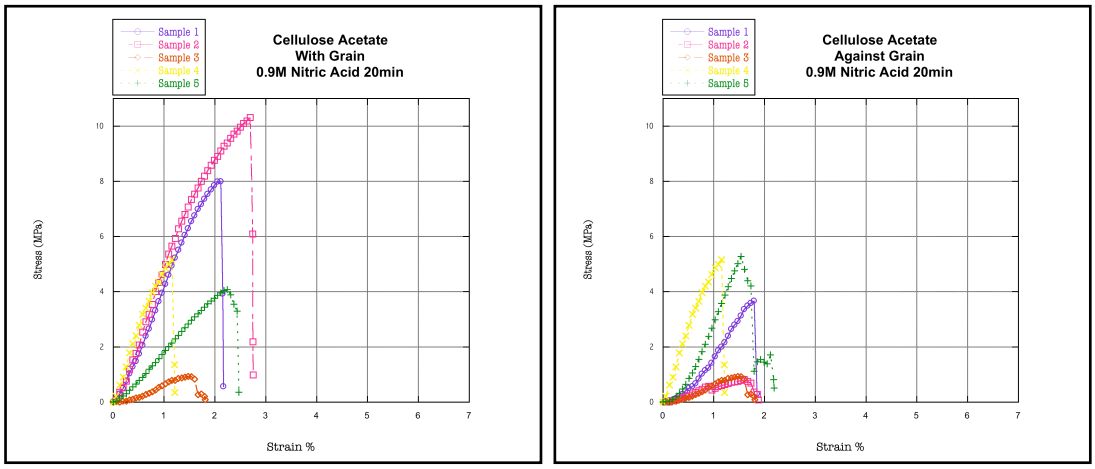

Figure 12: Graphs of tensile data of cellulose acetate after treatment with 0.9M nitric acid for 20 minutes with grain (a) and against grain (b).

During the most mild treatment option, 20 minute exposure to 0.9 M nitric acid, a new phenomena begins to appear in the break behavior: specifically, the appearance of semi-sharp breaks among weaker samples (Figure 12). Previously, with no treatment, the shape of the stress vs strain curve showed a clean break in all cases (Figure 11). However, after this treatment two samples with the fiber grain (samples 3 and 5) and three samples against the fiber grain (samples 2, 3, and 5) exhibit a change in the nature of their breakpoints. In these cases, there is still a clear break point, but rather than exhibiting a loss of nearly all strength at once, the samples lose tensile strength at random intervals. This suggests breaking as smaller, separate entities rather than one continuous whole as before. Also, in these cases, a decrease in both the young's modulus and force at break is also observed. As stated previously, this could possibly be explained by the treatment being too mild to increase fiber bonding while still being strong enough to decrease the integrity of the fibers in some cases.

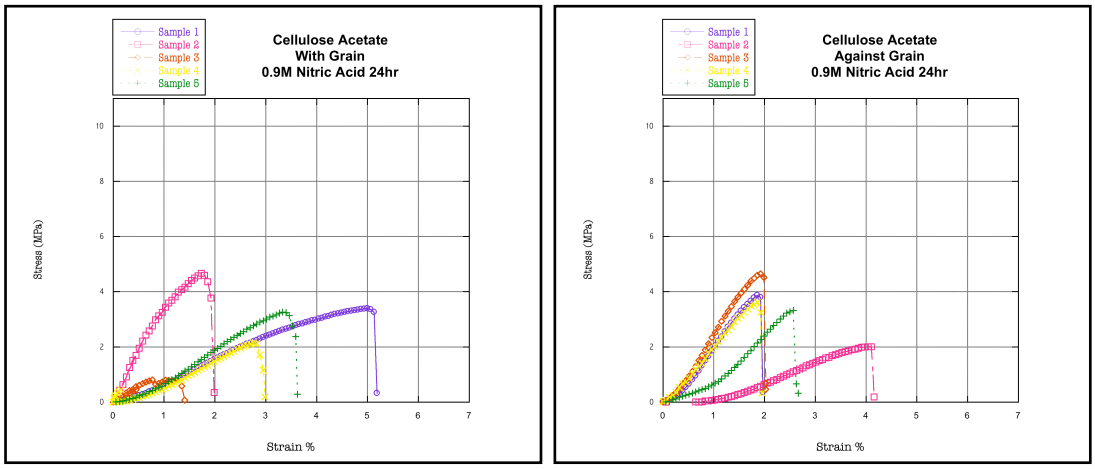

Figure 13: Graphs of tensile data of cellulose acetate after treatment with 0.9M Nitric Acid for 24 hours with grain (a) and against grain (b).

In the case of the 24 hour treatment of 0.9 nitric acid, both completely sharp and semi-sharp breakpoints are observed (Figure 13). Also, similarly to the no treatment option, each grouping seems to form a specific trend which one sample on the graph does not follow. In this case, however, this trend seems to be in the young's modulus (as visible by the linear portion of each curve). All but one sample (sample 2) among the samples cut with the grain exhibit a young's modulus close to 0.8 MPa stress per percent strain, whereas all but one sample (sample 2, again) cut against the grain group around 2.5 MPa stress per percent strain. Intriguingly, the breakpoints in both groupings are semi-sharp in all cases. This suggests that whatever is changing the nature of the breakpoints, may not have a direct correlation on the young's modulus of the material. In other words, though the treatment may be changing the nature of the break, it is not strengthening or weakening the material in the process. This treatment may, however, be changing the elasticity. Sample 5 cut with the grain and sample 2 cut against the grain exhibit the largest strain percent before breaking up to this point.

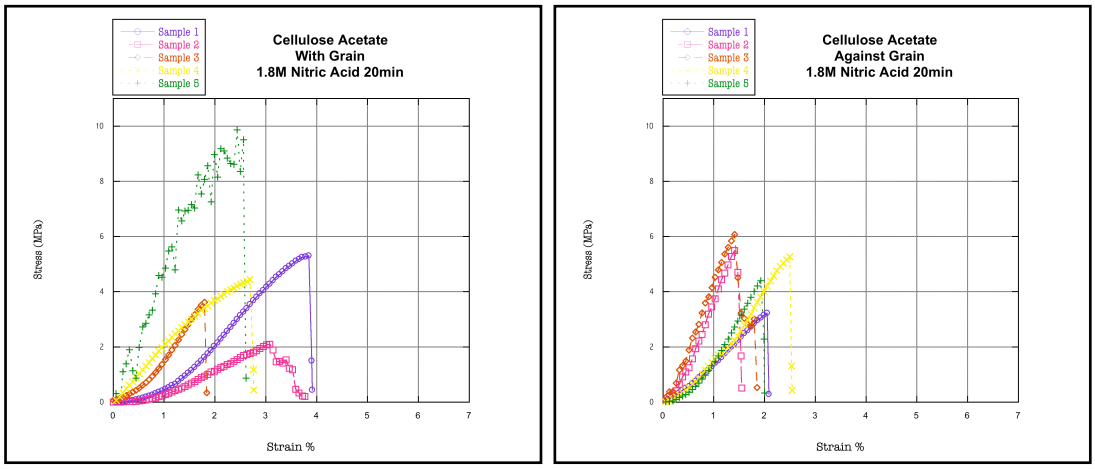

Figure 14: Graphs of tensile data of cellulose acetate after treatment with 1.8M Nitric Acid for 20 minutes with grain (a) and against grain (b).

With the introduction of the harsher acid treatment of 1.8M nitric acid, even for a short time of 20 minutes (Figure 14), yet another new break behavior is observed. Two samples cut with the grain present completely unique break behavior; sample 5 shows erratic behavior in the smoothness of its stress vs strain curve itself, and sample 2 shows the most drastic semi-sharp loss in strength yet. All other cases, both with and against the grain, exhibit sharp break points. This data suggests that the harsher treatment may be weakening the bonds between fibers in some samples (samples 2 and 5 with the grain), while simultaneously more strongly bonding all the others.

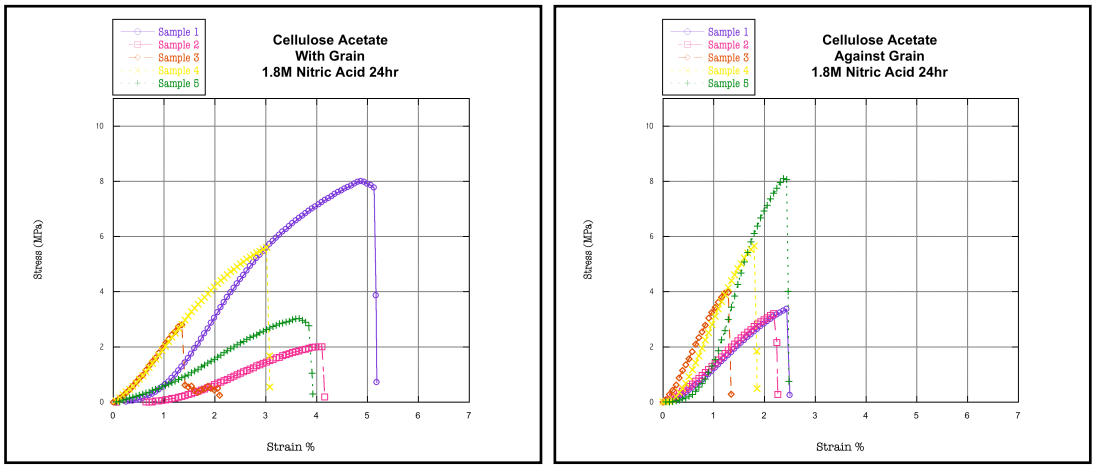

Figure 15: Graphs of tensile data of cellulose acetate after treatment with 1.8M Nitric Acid for 24 hours with grain (a) and against grain (b).

Finally, the harshest nitric acid treatment of 1.8M for 24 hours presents an intriguing range of results. The samples cut both with and against the grain exhibit a wide range of both stresses and strain percentages at the breakpoints. All breakpoints are either semi-sharp (samples 1 and 5 cut with grain) or sharp (all others with or against grain). In addition, there seems to be two groupings of the young's modulus in each graph. Among the samples cut with the grain, three (samples 1, 3, and 4) have a young's modulus grouped around 2.3 MPa per percent strain, while the other two (samples 2 and 5) have a young's modulus around 0.8 MPa per percent strain. Conversley, three of the samples cut against the grain (samples 3, 4, and 5), have a young's modulus grouped around 5 MPa per percent strain, while the remaining two (samples 1 and 2) have a young's modulus around 1.6 MPa per percent strain.

Cellulose Nitrate

As with cellulose acetate, none of the treatments tested produced a statistically significant change in the extension at break (Figure 17) or the force to break (Figure 18), suggesting that the overall morphology of the samples was maintained. However, there was a significant change in the young's modulus of one of the treatments (Figure 16). In the case of the harshest acetone treatment tested with the grain, a 24 hour submersion of 1:9 (v:v) acetone to water, an average young's modulus of more than twice that of the untreated sample was observed. This is likely due to an increase in the bonds between the fibers at this treatment level.

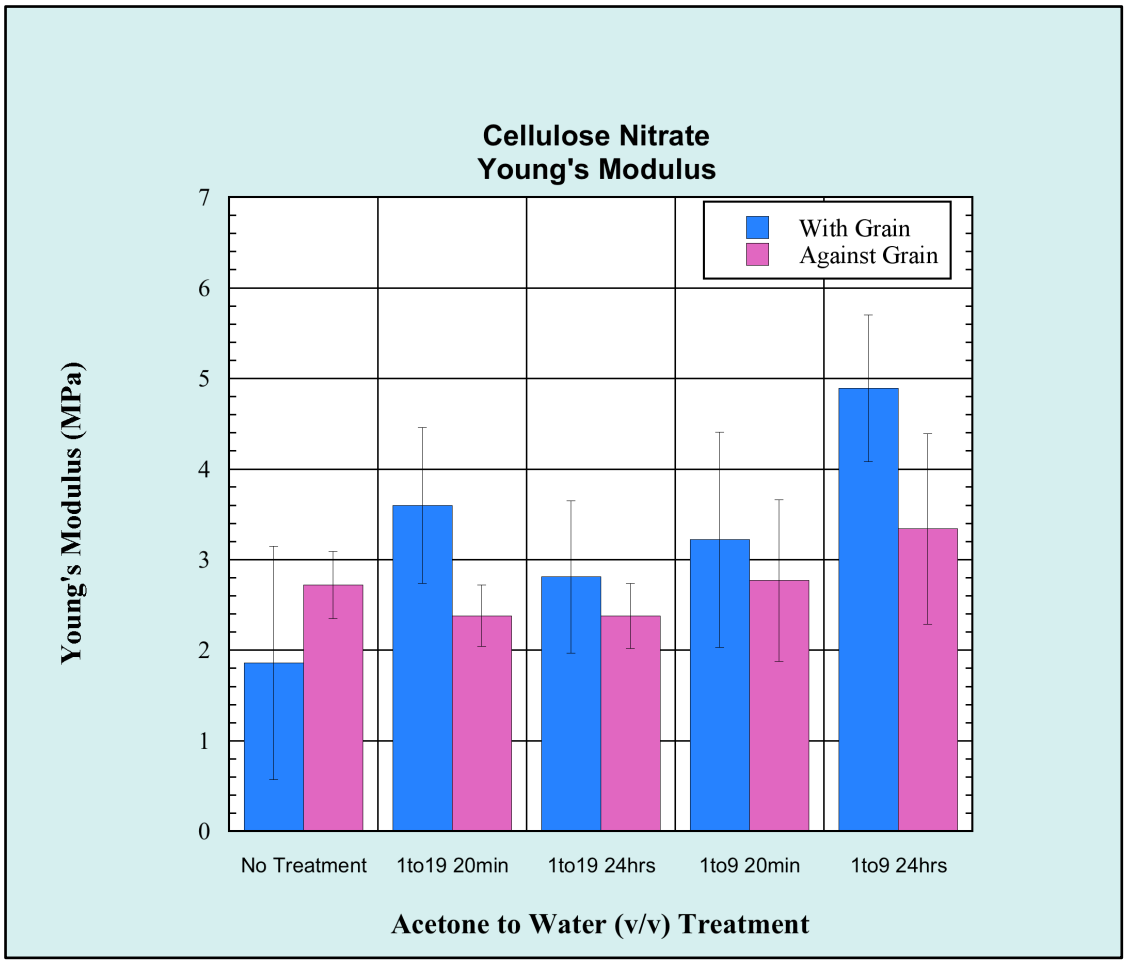

Figure 16: Young's Modulus data for cellulose nitrate.

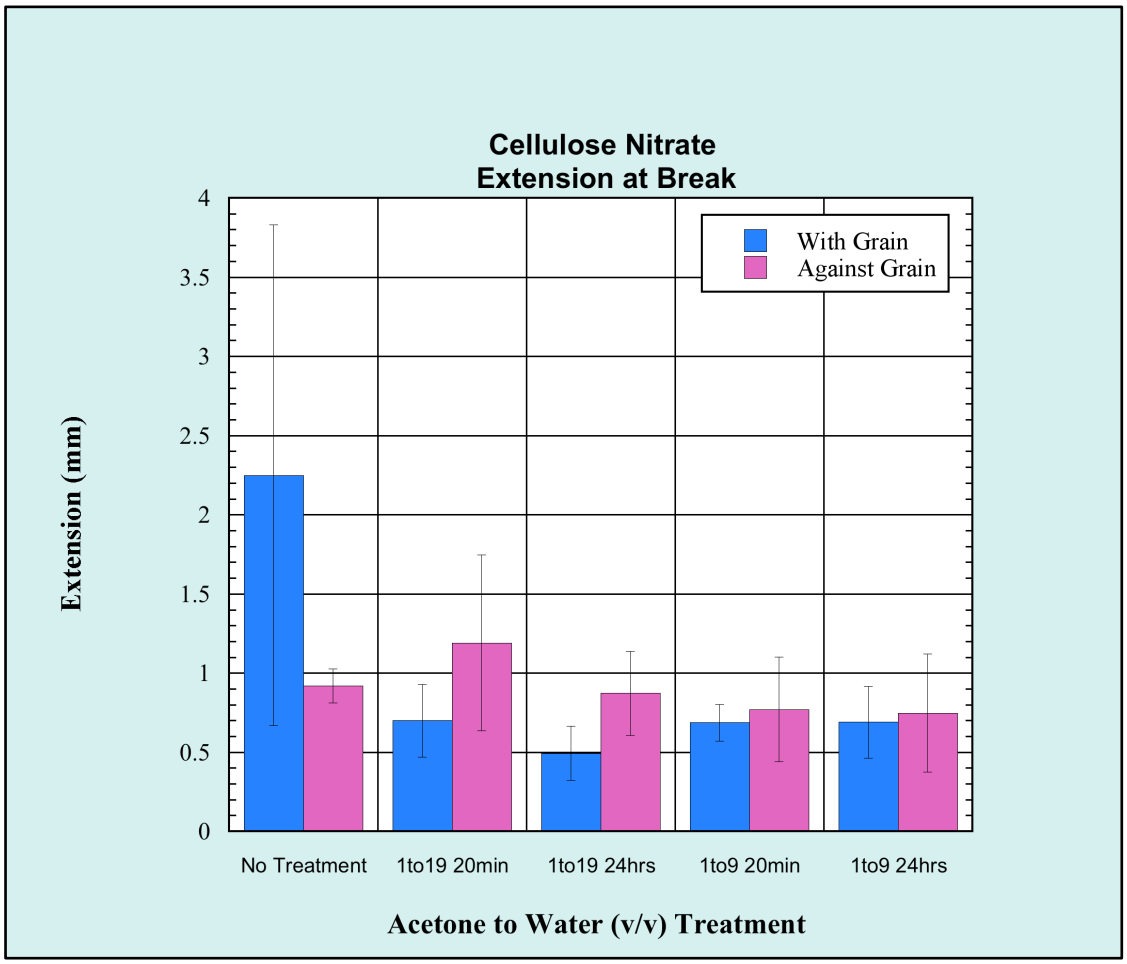

Figure 17: Extension at break data for cellulose nitrate.

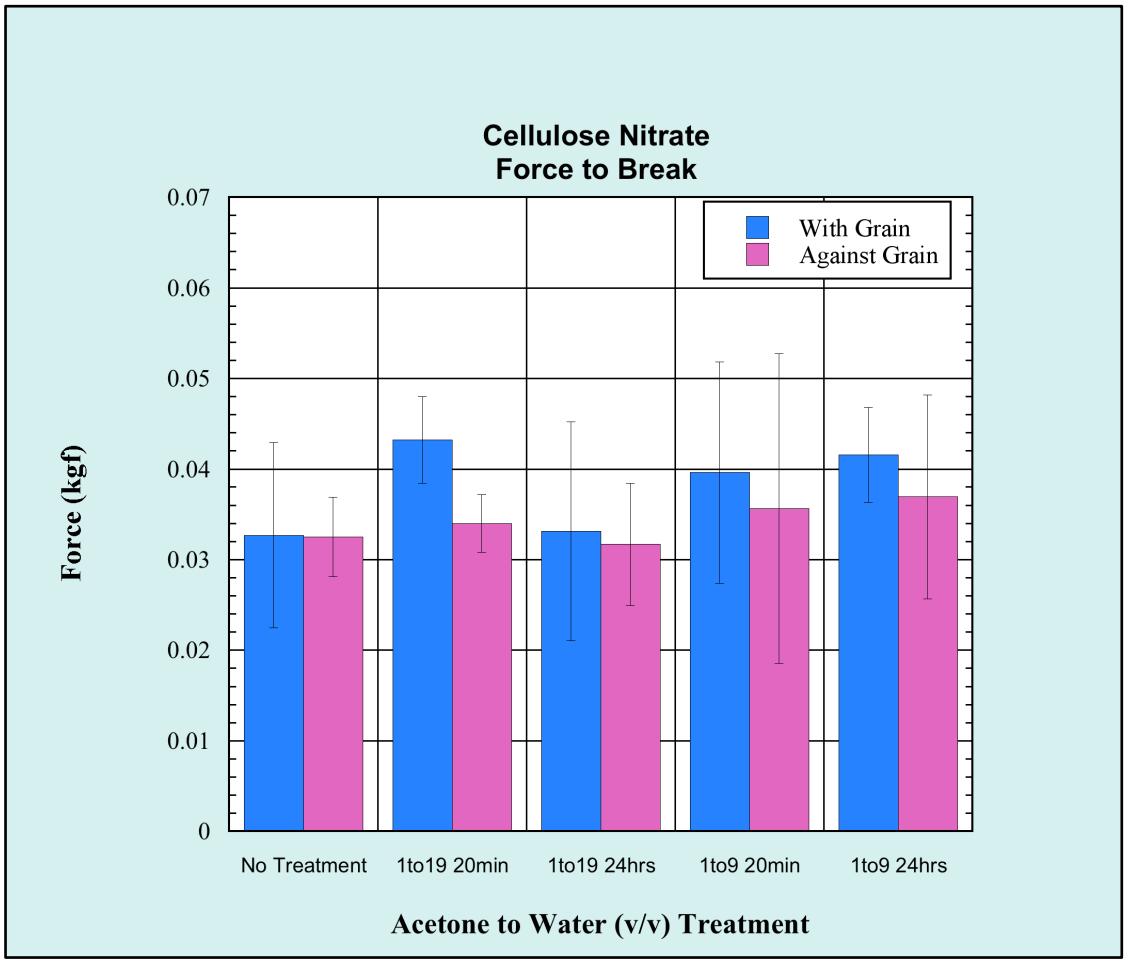

Figure 18: Force to break data for cellulose nitrate.

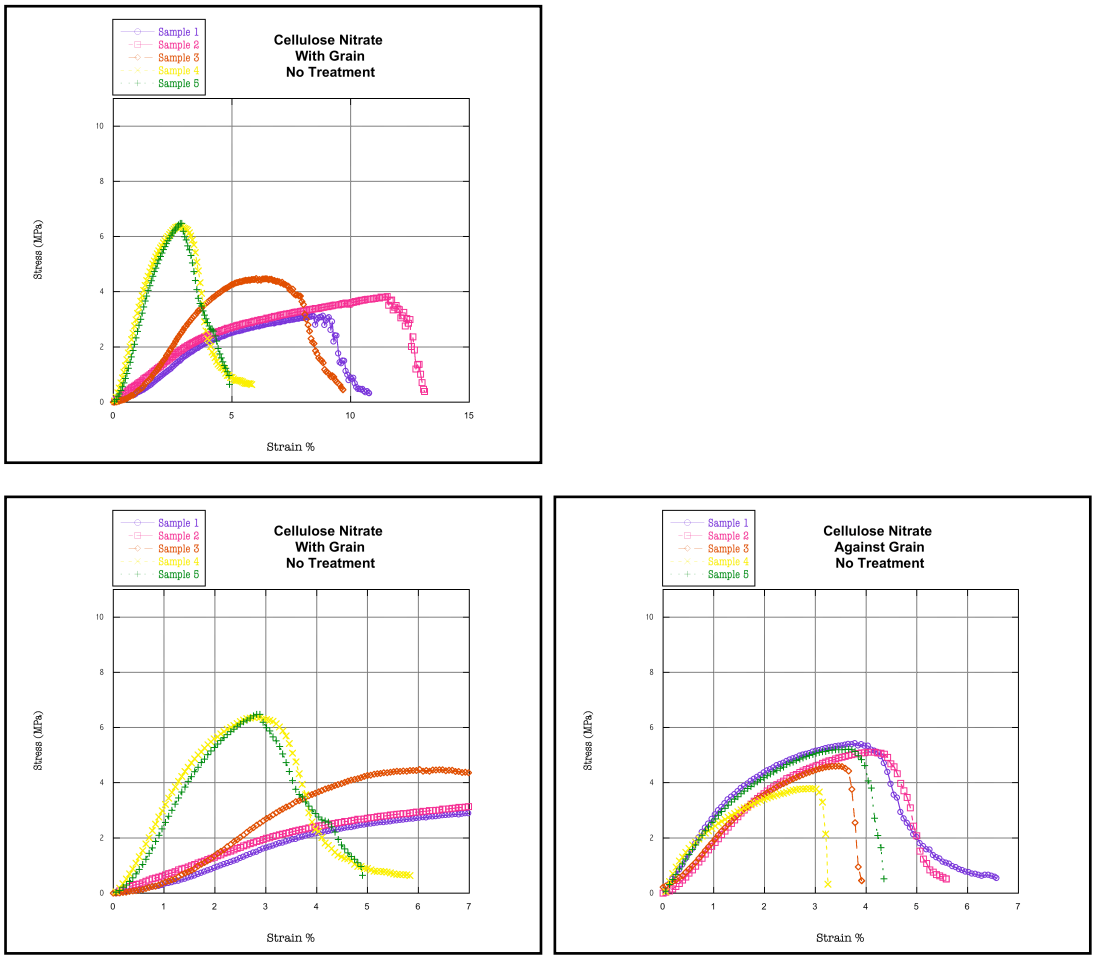

Figure 19: Graphs of tensile data of cellulose nitrate before treatment with grain zoomed out (a1), with grain zoomed in (a2), and against grain (b). In order to view all stress vs strain curves on the same axis (thus making them easier to compare directly), a zoomed out and a zoomed in version was made of the tensile data representing no treatment samples cut with the grain. The zoomed out version shows all of the data collected, whereas the zoomed in version presents most of the relevant data on the same axis as all other stress vs strain curves throughout this work.

In the case of the cellulose nitrate samples tested without any treatment (Figure 19), every sample both with and against the grain exhibited a break point in the plastic region of the stress vs strain curve, as apparent by the concavity of the graph at the breakpoint. This shows that the mats are strain hardening and ductile. In addition, no sample exhibited a sharp break as had been observed initially with cellulose acetate. Instead, samples broke gradually, suggesting that the fibers break separately rather than the mat breaking as one coherent piece. For the samples cut with the grain, a staggering range of break characteristics is

present; both in the shape of the curves themselves (from asymmetrically drawn out to almost parabolic in shape) and the stress (from approximately 3 MPa to greater than 6 MPa) or strain (from less than 3 % to more than 12%) at the break point. It is not easily apparent why this would be the case. Perhaps these large differences are due a variation of fiber-fiber interaction or entanglement between samples caused from the spinning conditions. This explanation would allow for these large ranges, yet still be consistent with gradual breaks resulting from the breaking of individual fibers rather than the mat as one coherence piece.

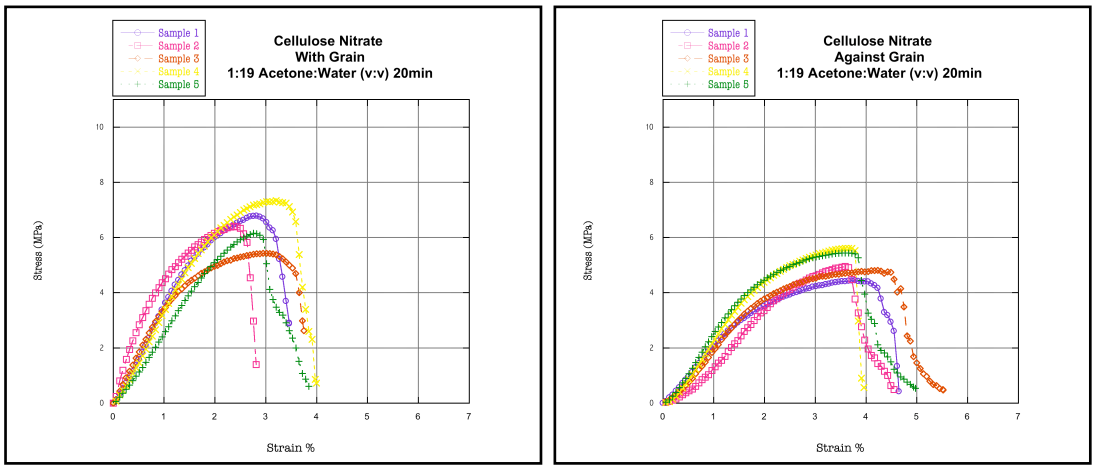

Figure 20: Graphs of tensile data of cellulose nitrate after treatment with 1:19 (v:v) acetone:water for 20 minutes with grain (a) and against grain (b).

Unlike untreated cellulose nitrate, the mildest treatment of cellulose nitrate, 1:19 (v:v) acetone to water for 20 minutes, yields closely clustered results both with and against the grain (Figure 20). Once again, the breaks are consistent with the plastic region of the curve. In addition, the young's modulus for both graphs forms clusters, about 3.5 MPa per percent strain for samples cut with the grain and about 2.5 MPa per percent strain for samples cut against the grain. This data suggests a slight presence of anisotropic break behavior; the strength of the mats cut with the grain may be reliant slightly more on the strength of the individual fibers whereas that of the mats cut against the grain

may be reliant on the weaker interactions between the fibers. This would account for the higher young's modulus, higher stress at the breakpoints, and lower strain percentage at the breakpoints.

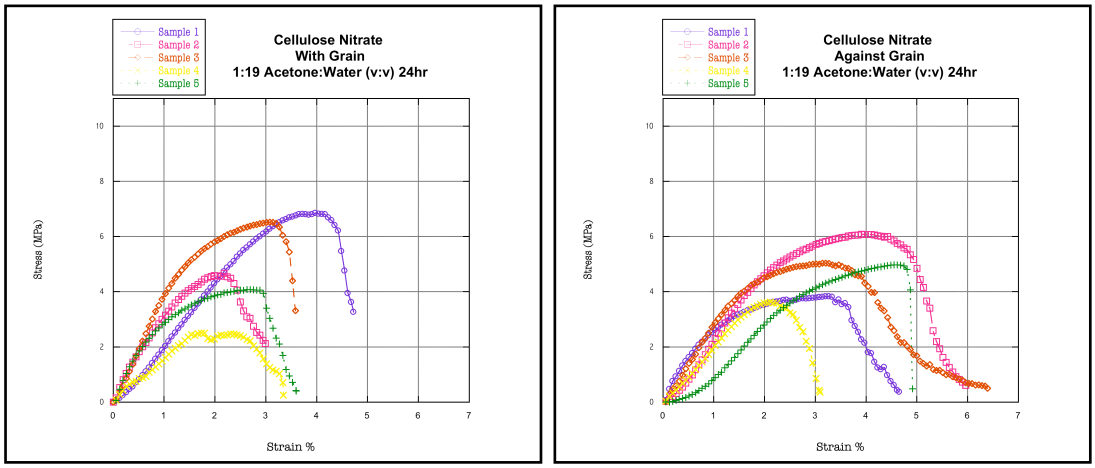

Figure 21: Graphs of tensile data of cellulose nitrate after treatment with 1:19 (v:v) acetone:water for 24 hours with grain (a) and against grain (b).

As treatment time is increased from 20 minutes to 24 hours for 1:19 (v:v) acetone to water (Figure 21), a new type of break type begins to emerge with cellulose nitrate: the sharp break. Although only present in one sample (sample 5, against grain), this shows a marked change in the nature of the mats and the way that the fibers are beginning to interact. While maintaining its ductility as a whole, apparent by the break in the plastic region once again, this sample also exhibits characteristics of increased coherence, apparent by the sharp rather than gradual loss in strength which was previously witnessed. In addition, two samples cut with the grain (sample 3 and sample 5), are also beginning to show signs of semi-sharp breaks.

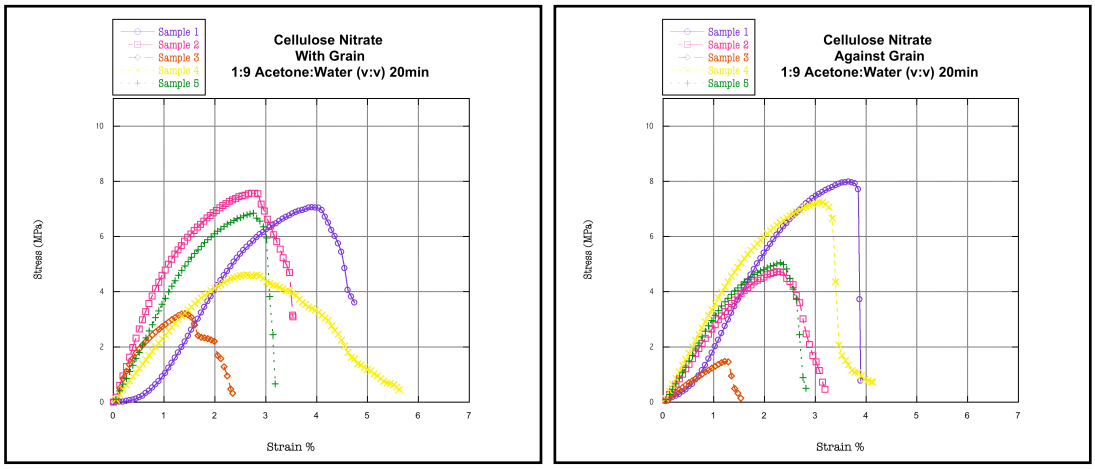

Figure 22: Graphs of tensile data of cellulose nitrate after treatment with 1:9 (v:v) acetone:water for 20 minutes with grain (a) and against grain (b).

Increasing the concentration and decreasing the time produces a similar result to the lower concentration at a higher time. After treatment of 1:9 (v:v) acetone to water for 20 minutes, the cellulose nitrate again exhibits a mixture of break types ranging from gradual (for example sample 4, with grain) to semi-sharp (for example sample 1, against grain). This once again suggests an increase in fiber bonding in some samples which had not been present before treatment or in the mildest treatment. It is also interesting to note that this treatment also includes the cellulose nitrate sample with the lowest stress and strain values tested thus far (sample 3, with grain). Since this sample exhibits a semi-sharp break, this data suggests that increasing the cohesion of the mats may not necessarily increase the overall strength of the mats. Instead, this increased fiber-fiber bonding may merely change the nature of the break.

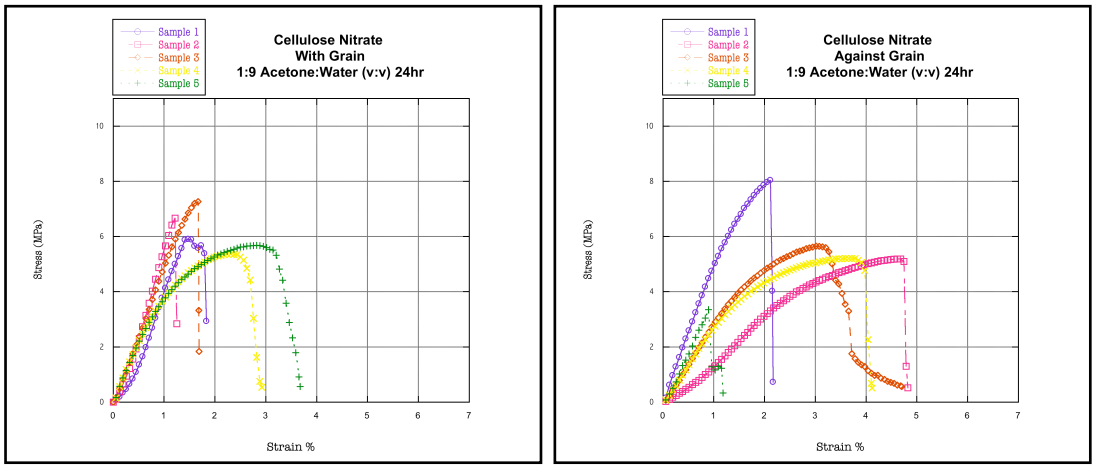

Figure 23: Graphs of tensile data of cellulose nitrate after treatment with 1:9 (v:v) acetone:water for 24 hours with grain (a) and against grain (b).

Finally, with the harshest treatment tested, 1:9 (v:v) acetone to water for 24 hours, yet another break type emerges: the truly sharp break (Figure 23). This type of break is present both in the elastic region (samples 2 and 3, with grain, and sample 5, against grain) and plastic region (samples 1, 2, and 4, against grain) of the stress vs strain curve, showing that the mats are now presenting both brittle and ductile characteristics. In addition, semi-sharp breaks are also present in the remaining samples, a phenomena which had not been present after previous treatments. This drastic change in the nature of the breaks after the strongest treatment with acetone presents compelling evidence that indeed additional bonding between the fibers has taken place, thus casing the mats to break as one coherent piece rather than a loose bundle of fibers.

Fourier Transform Infrared Spectroscopy (FTIR)

For this study, FTIR spectra (Figure 24) were taken to both confirm the chemical structure of each starting material and also to illuminate any changes in the structure of the cellulose acetate after treatment with nitric acid. In this study, two peaks were used to confirm and study changes in the presence of substituted functional groups on the cellulose: 1738 cm^{-1} was examined to determine the presence of acetate and 1639 cm^{-1} was examined to determine the presence of nitrate. As would be expected, the spectrum of cellulose nitrate exhibits a strong peak at 1639 cm^{-1} to correspond to a high substitution of nitrate and nearly no peak at 1738 cm^{-1} to correspond to nearly no presence of acetate. Conversely, both the treated and untreated spectra of cellulose acetate exhibit a weak peak at 1639 cm^{-1} corresponding to a low presence of nitrate and a strong peak at 1738 cm^{-1} to correspond to a high presence of acetate. This is to be expected, even after nitration, because the mild nitration conditions should have only caused substitution on the surface of the fibers, leaving the majority of the acetate fully intact.

To further support the supposition that nitration was indeed present on the surface of the fiber, increasing the overall nitration only slightly, the peak heights of the acetate peak relative to the nitrate peak were examined (Figure 25). This is not a direct measure of the degree of substitution for each functional group, because the heights of the peaks to not increase in the same way among different functional groups. However, this does show a statistically significant increase in the height of the peak corresponding to the presence of nitrate relative to the peak corresponding to the presence of acetate, suggesting that some nitration is in fact occurring in the sample.

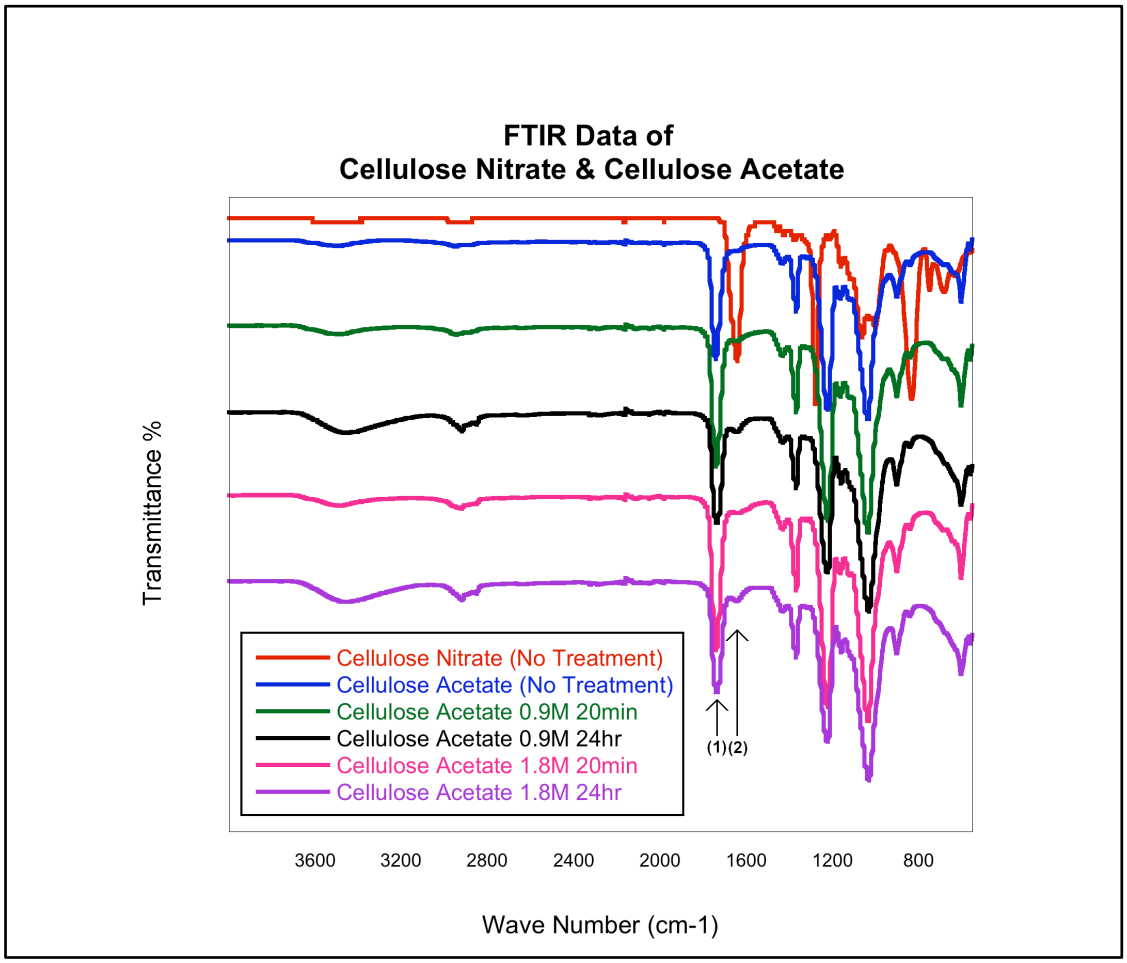

Figure 24: FTIR data of cellulose nitrate and cellulose acetate. To show each spectrum relative to the others, the percent transmittance values were shifted. The peaks which were examined most closely to determine the presence of (1) acetate and (2) nitrate groups are 1738 and 1639 cm^{-1} respectively.

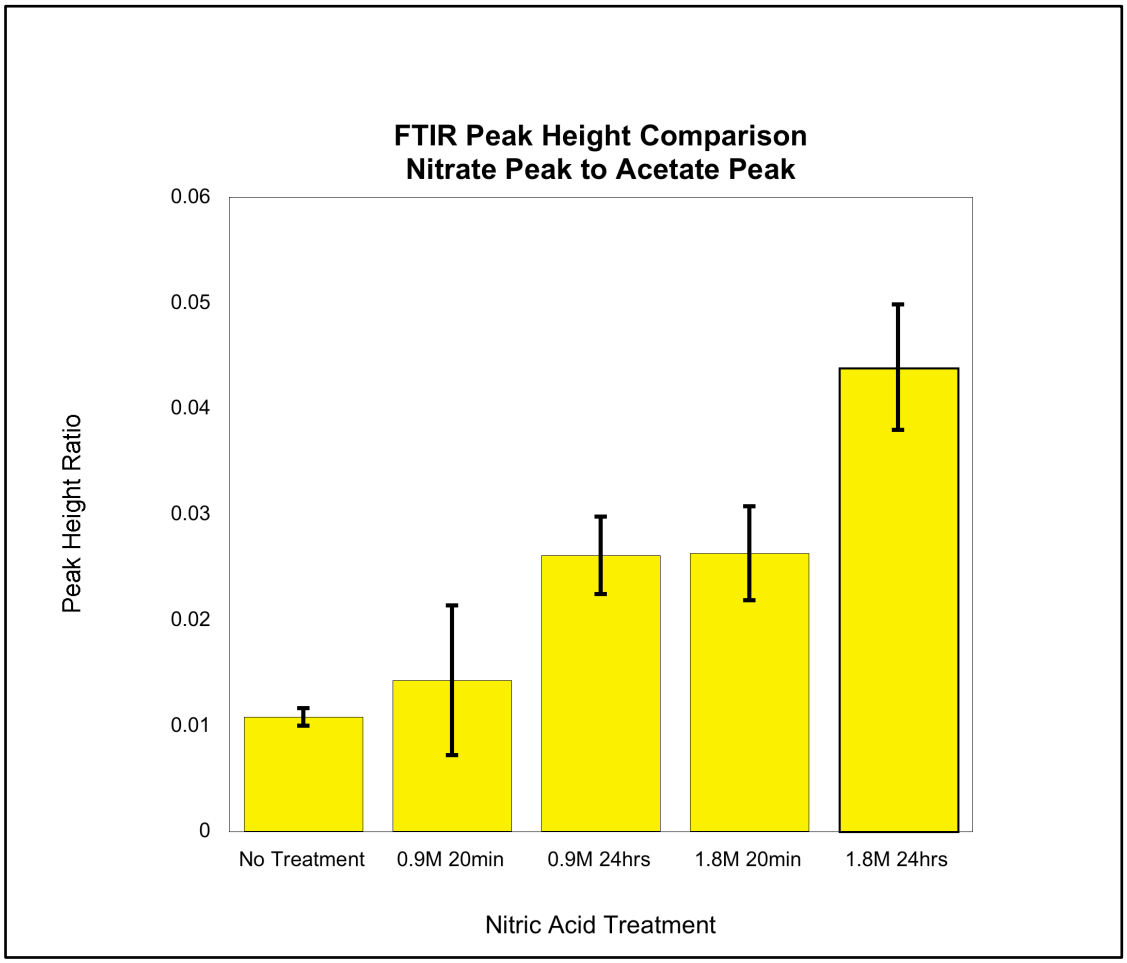

Figure 25: FTIR peak height comparison of cellulose nitrate after various treatments with nitric acid. Each value was determined by taking the relative peak height of the acetate peak at 1639 cm-1 and dividing it by the relative peak height of the nitrate peak at 1738 cm-1.

X-Ray Photoelectron Spectroscopy (XPS)

In addition to FTIR, which gives insights into the chemical structure of the bulk material, XPS was also performed to determine elemental composition at the surface (Figure 26, Table 4). As with FTIR, which suggested a significant presence of nitrogen in the untreated cellulose nitrate, XPS showed an approximately 10.1% presence of nitrogen at the surface. Conversely, XPS found no nitrogen at the surface of both treated and untreated cellulose acetate. In this case, surface concentrations of oxygen and carbon did show a change before and after treatment, suggesting that a chemical reaction did occur; this reaction, however, does not appear to be nitration.

Table 4: Surface Percent of Oxygen, Carbon, and Nitrogen as Determined Through XPS.

	Oxygen	Carbon	Nitrogen
Cellulose Nitrate (No Treatment)	43.2%	46.6%	10.2%
Cellulose Acetate (No Treatment)	36.5%	63.5%	0.0%
Cellulose Acetate 1.8M 24hr	32.4%	67.6%	0.0%

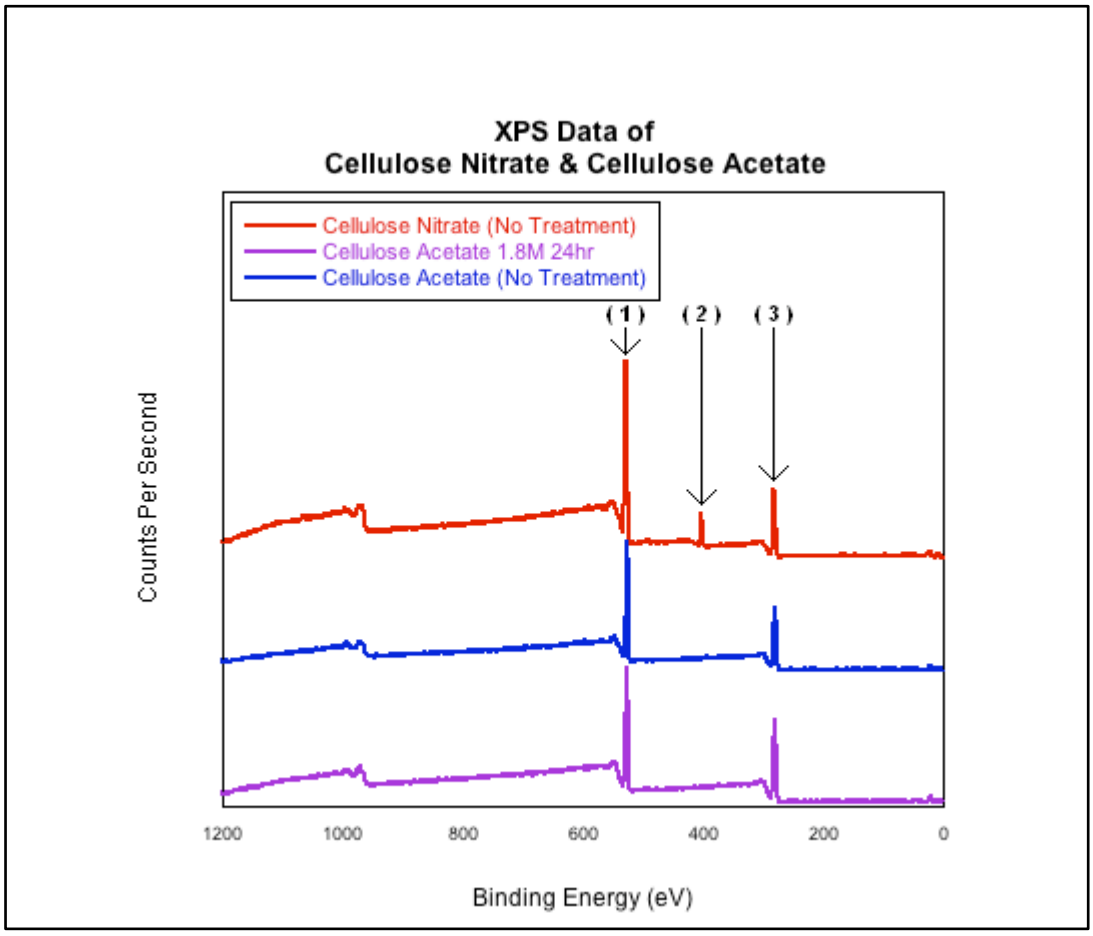

Figure 26: XPS data of cellulose nitrate and cellulose acetate. To show each spectrum relative to the others, the counts per second values were shifted. The binding energy peaks which were examined most closely to determine the percent of (1) oxygen, (2) nitrogen, and (3) carbon at the surface are 582 eV, 403 eV, and 282 eV respectively.

Scanning Electron Microscopy (SEM)

Cellulose Acetate

Even without treatment, there is little to distinguish the images of the nanofiber mats made of cellulose acetate as being with or against the spinning grain, suggesting that the material is largely isotropic. In the low magnification image (Figure 27), the samples subjected to no treatment and cut both with and against the grain exhibit fibers with relatively random orientation connected in a random, web-like network. At many intersections of fibers, clear connections between fibers can be seen. This is

also clearly visible on the high magnification images (Figure 28). When examining the breaks of individual fibers in these images, jagged breaks perpendicular to the length of the fiber are present. In addition, fibrillation of the larger fibers into smaller fibers (center of lower image) is also present.

After even the mildest treatment, changes in the interactions of the fibers can already be seen. Upon examining the low magnification images of samples after 20 minute treatment with 0.9M nitric acid (Figure 29), amorphous patches of polymer are present in the top image, likely formed by clusters of fibers which have melted together during the nitration process. These patches may work to bind together the remaining fibers more strongly than the original connections at fiber-fiber intersections, which were present without treatment. As with no treatment, the high magnification images (Figure 30) show the same jagged breaks of the fibers within the networks.

As the length in time for treatment increases from 20 minutes to 24 hours for 0.9M nitric acid, so increases the change in the morphology of the mat. In the low magnification images (Figure 31), the degree of networking is so great that individual fibers cease to exist in places (particularly, the top left corner of the lower image). This networking does not seem to largely effect the breakpoints of mat in the zoomed in images, however (Figure 32): jagged breaks are still present.

As with the milder treatments, harsher treatment conditions of 20 minutes and 24 hours with 1.8M nitric acid exhibit amorphous sections of melted-together, networked fibers (Figure 33, Figure 35). However, in the case of the longer treatment time, the amorphous sections are significantly larger, leaving less of the fiber morphology intact. The zoomed in images of both these treatments (Figure 34, Figure 36) also show jagged breakpoints of the polymer.

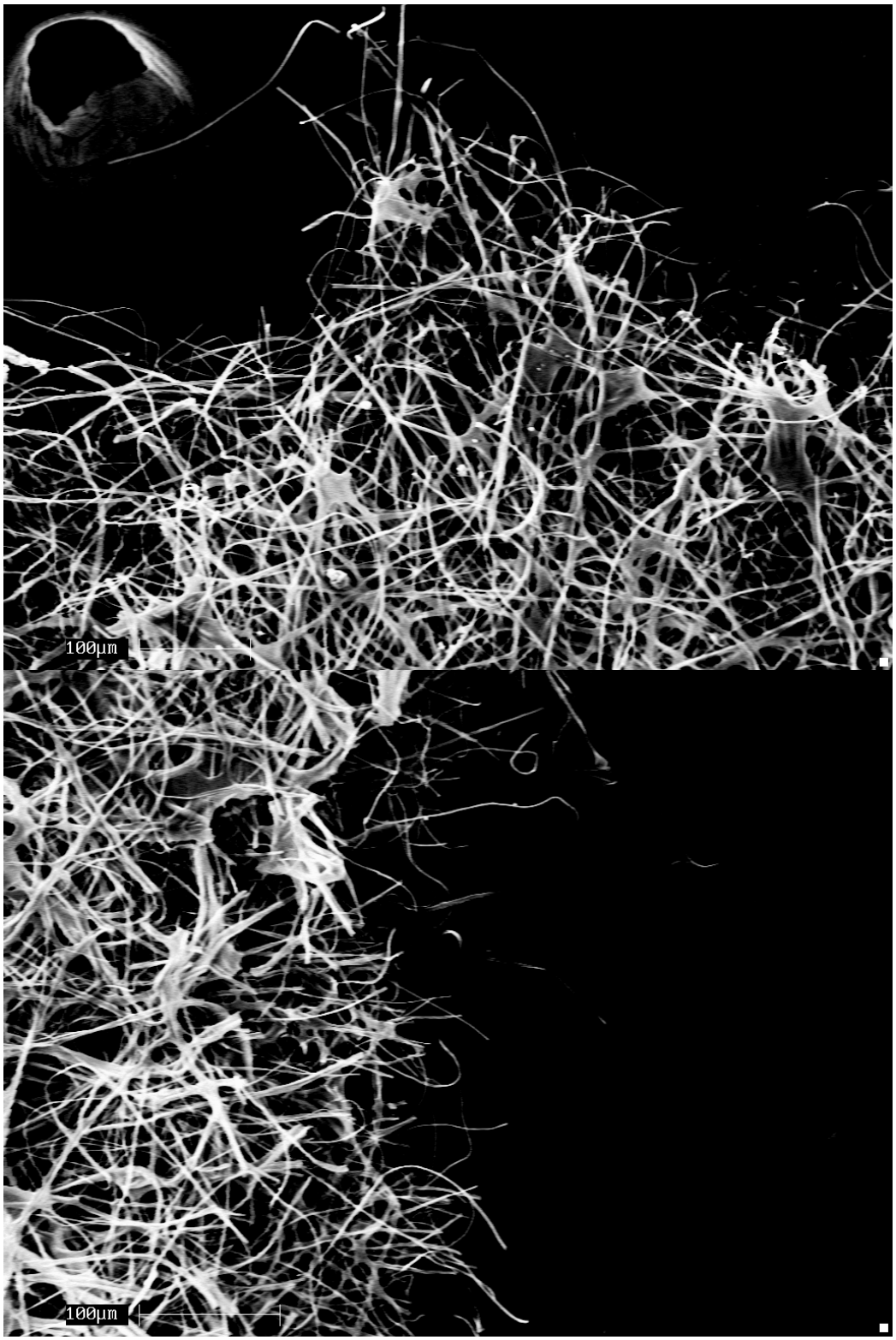

Figure 27: Low magnification SEM images of cellulose acetate with no treatment with grain (above) and against grain (below).

Figure 28: High magnification SEM images of cellulose acetate with no treatment with grain (above) and against grain (below).

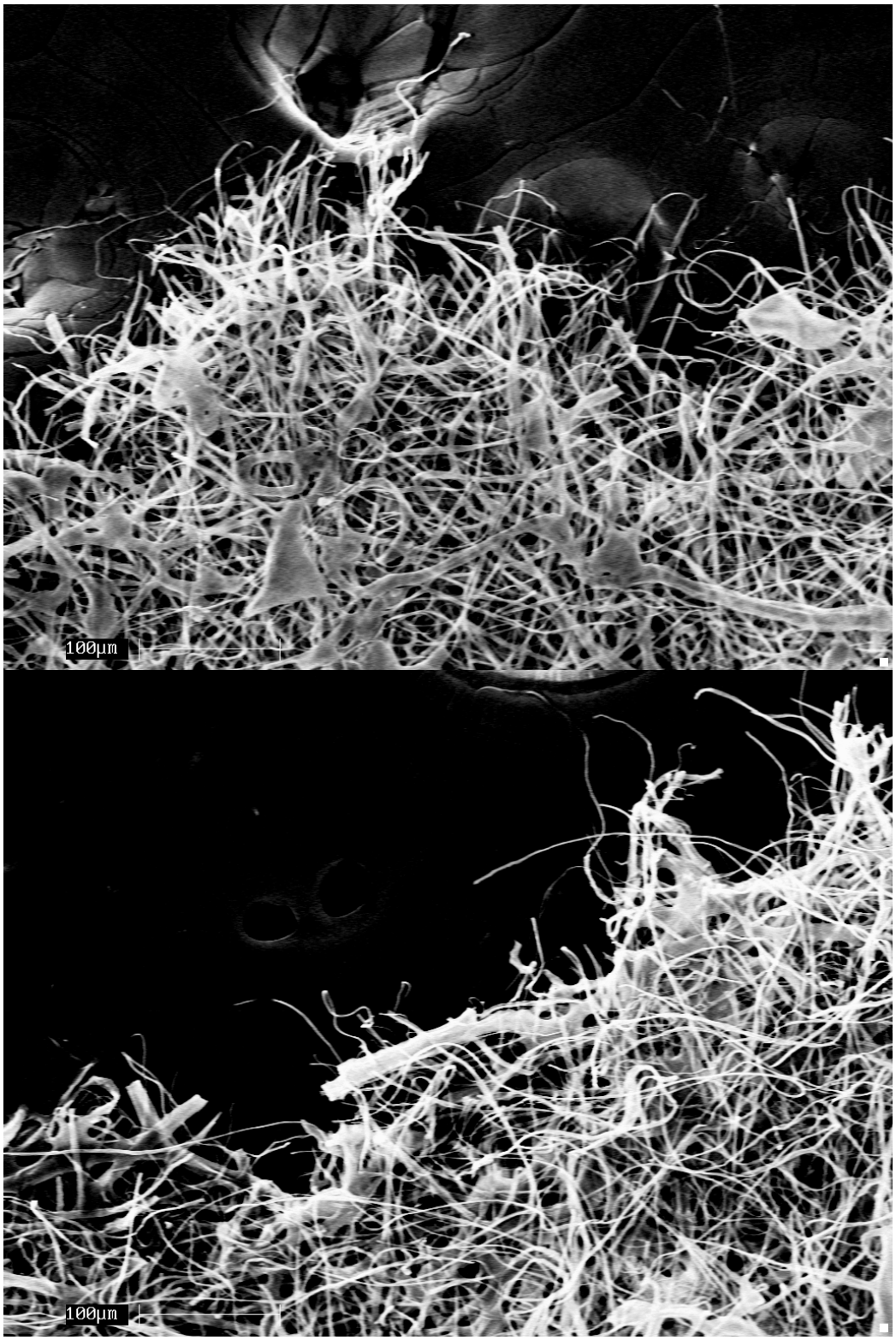

Figure 29: Low magnification SEM of cellulose acetate after treatment with 0.9M Nitric Acid for 20 minutes with grain (above) and against grain (below).

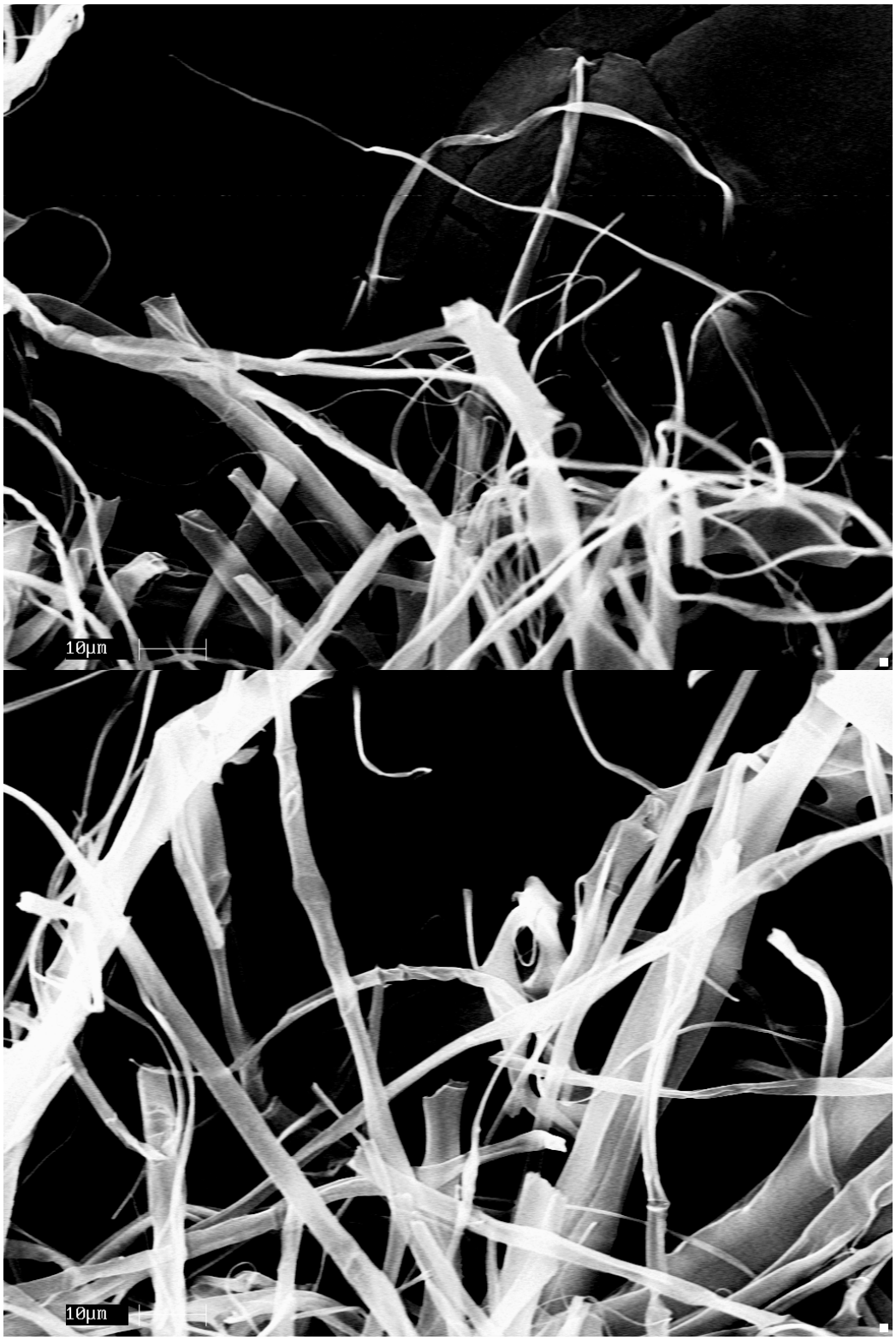

Figure 30: High magnification SEM of cellulose acetate after treatment with 0.9M Nitric Acid for 20 minutes with grain (above) and against grain (below).

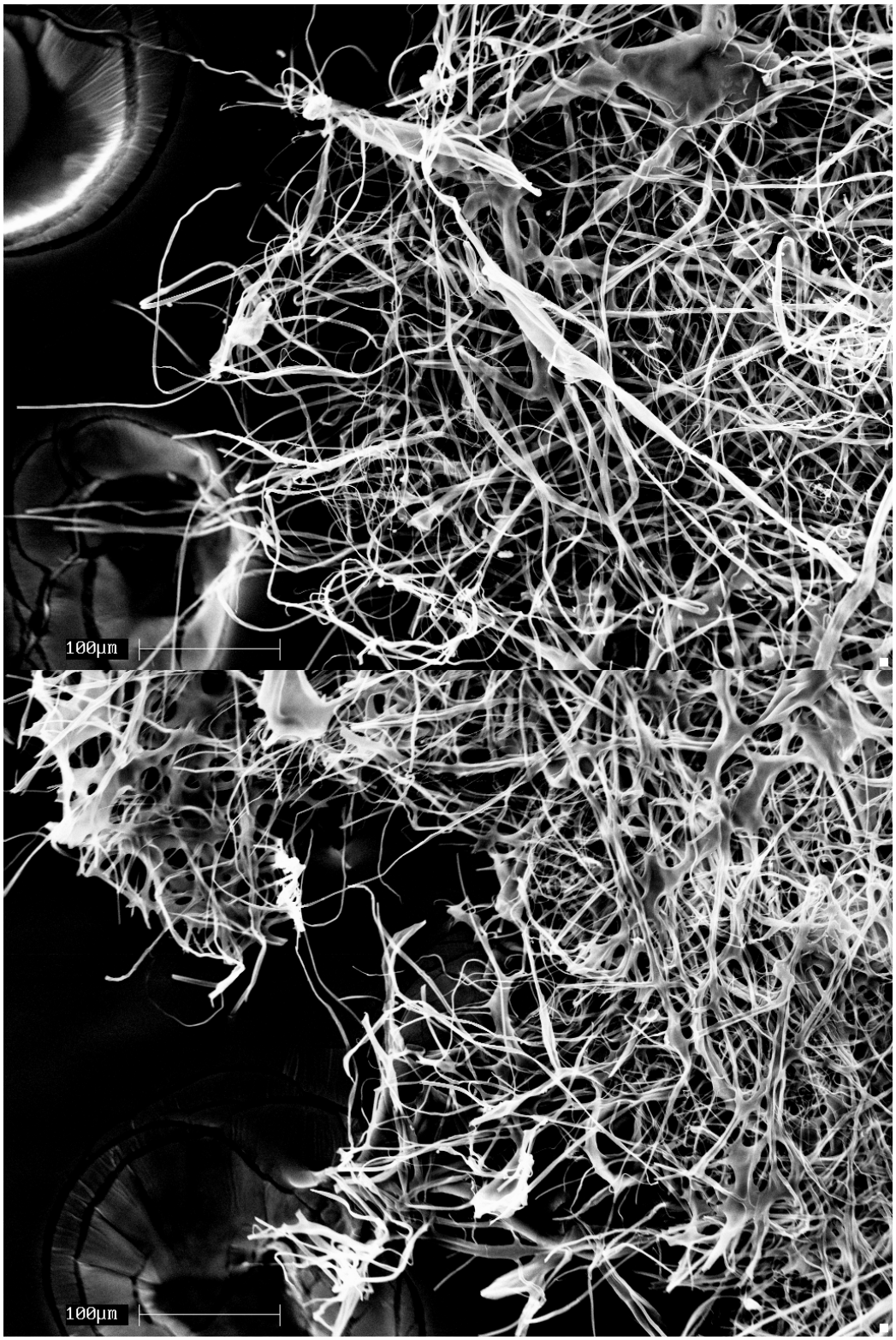

Figure 31: Low magnification SEM of cellulose acetate after treatment with 0.9M Nitric Acid for 24 hours with grain (above) and against grain (below).

Figure 32: High magnification SEM of cellulose acetate after treatment with 0.9M Nitric Acid for 24 hours with grain (above) and against grain (below).

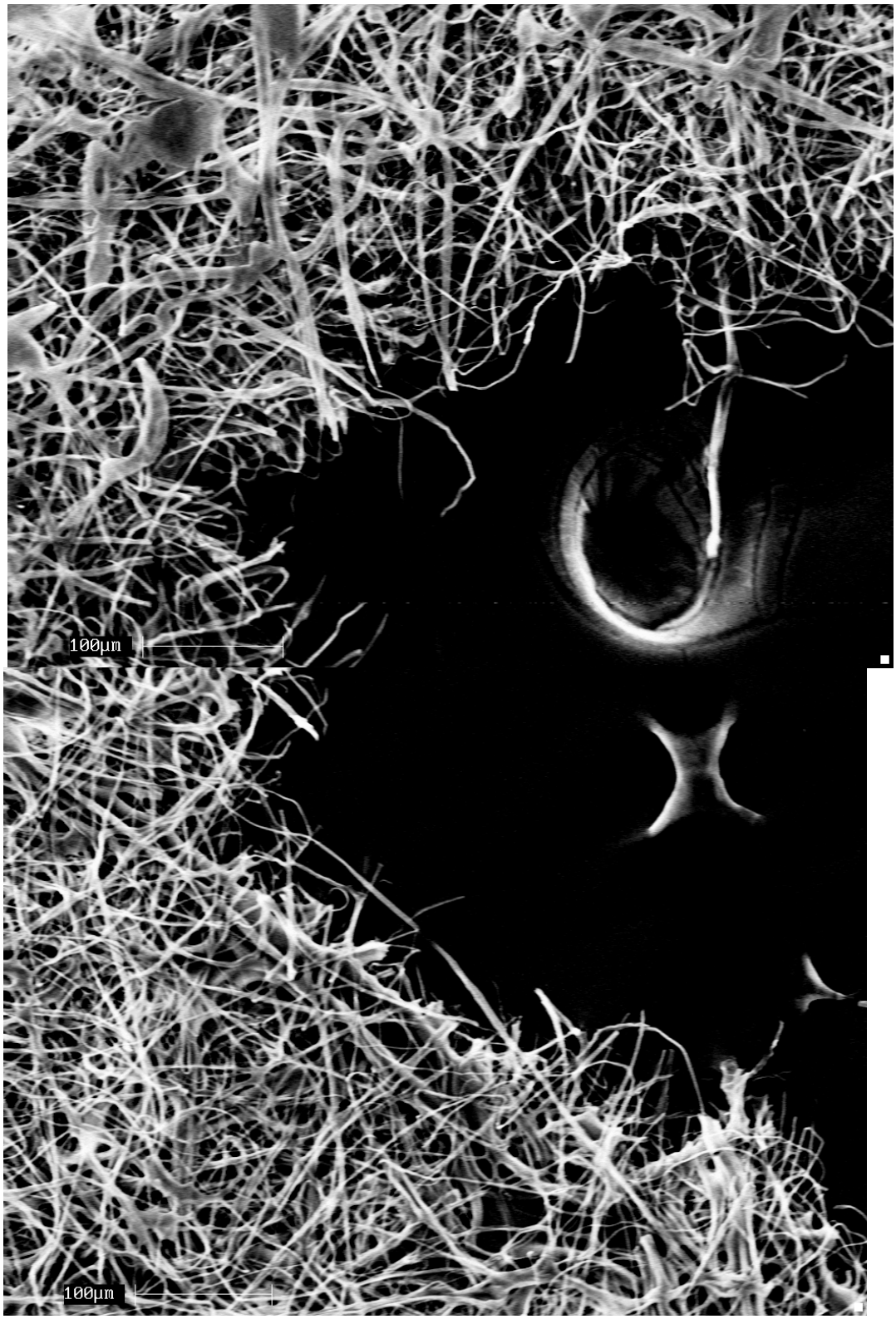

Figure 33: Low magnification SEM of cellulose acetate after treatment with 1.8M Nitric Acid for 20 minutes with grain (above) and against grain (below).

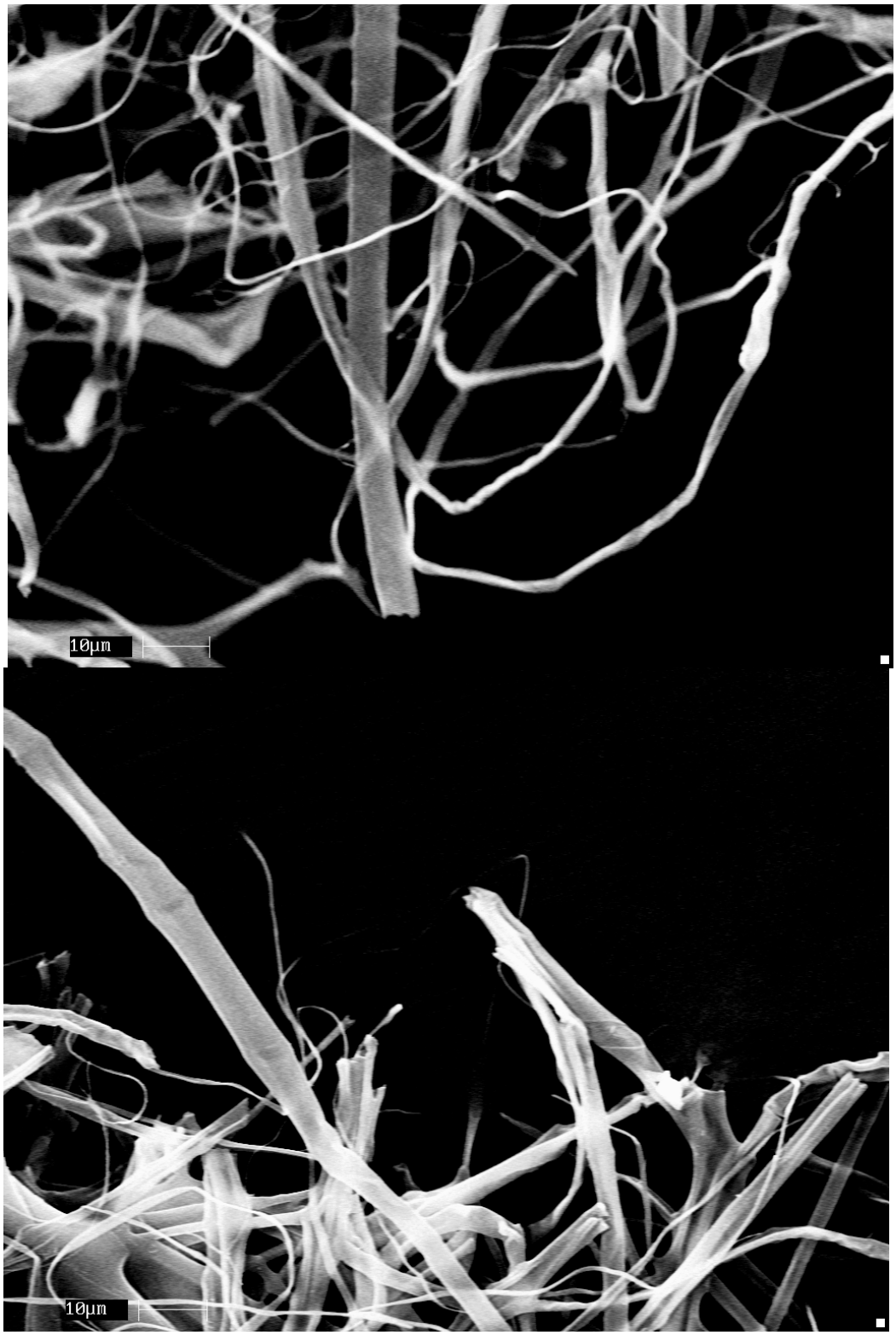

Figure 34: High magnification SEM of cellulose acetate after treatment with 1.8M Nitric Acid for 20 minutes with grain (above) and against grain (below).

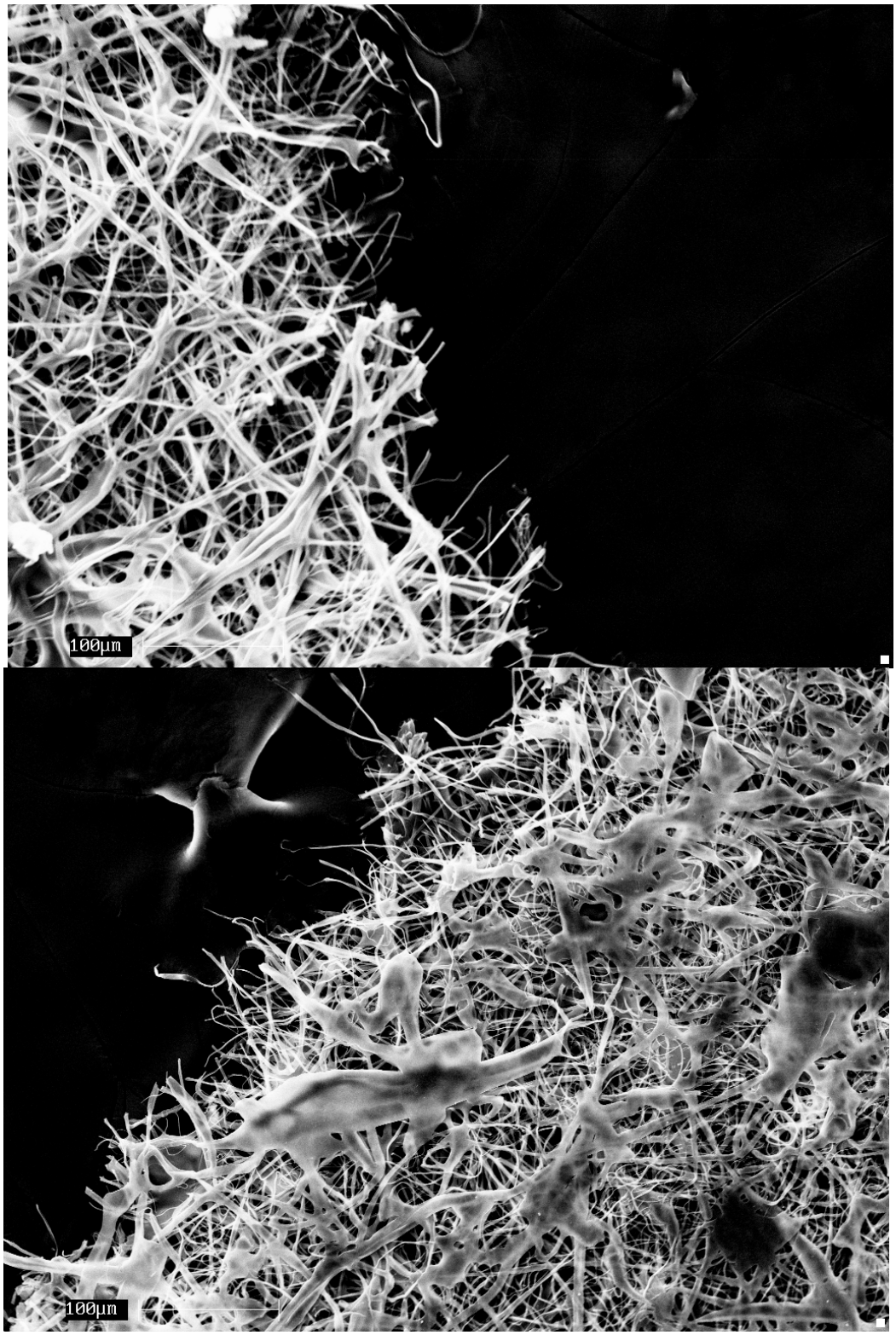

Figure 35: Low magnification SEM of cellulose acetate after treatment with 1.8M Nitric Acid for 24 hours with grain (above) and against grain (below).

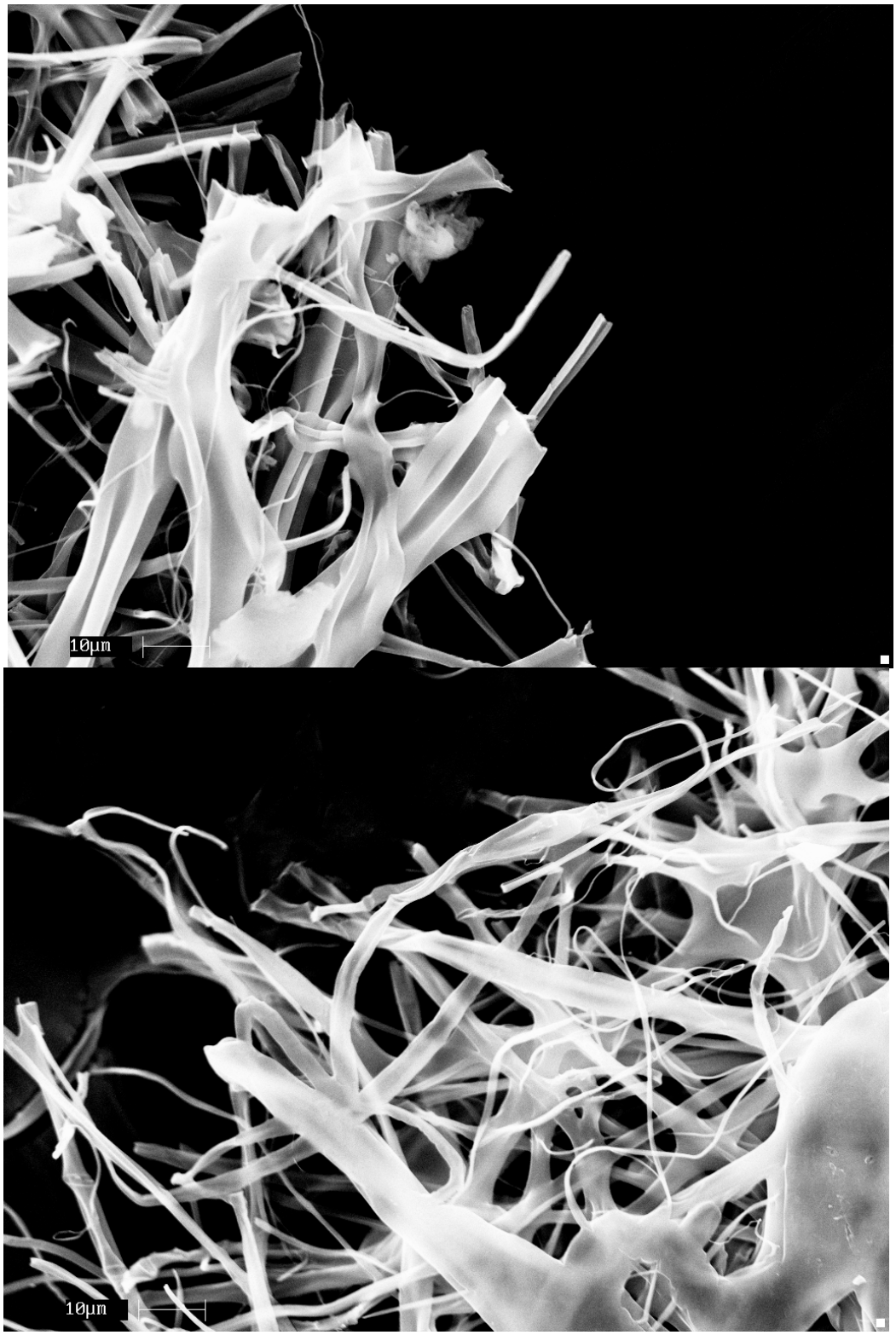

Figure 36: High magnification SEM of cellulose acetate after treatment with 1.8M Nitric Acid for 24 hours with grain (above) and against grain (below).

Cellulose Nitrate

Unlike cellulose acetate, which displayed evidence of cohesion between fibers even without treatment, the behavior of the cellulose nitrate mats is initially not cohesive. Based on the examination of the images with no treatment (**Figure 37**, **Figure 38**), the fibers are initially drawn parallel to the direction of stress before breaking, as evident by the orientation of the fibers close to the break point and lack of orientation of the fibers further from the break point. This behavior suggests that, without treatment, the strength of the interactions between the fibers is weaker than the fibers themselves, causing the fiber-fiber interaction to fail first.

Similar behavior is present after the mildest finishing treatment, exposure to 1:19 (v:v) acetone to water for 20 minutes. In the low magnification image (Figure 39), fibers can be seen which were drawn parallel to the strain, and in the high magnification image at the breakpoint (Figure 40), every fiber is oriented in this same direction.

As this treatment time is increased to 24 hours, however, a new phenomena begins to emerge. In the low magnification images (Figure 41), amorphous sections of polymer begin to appear dispersed among the fiber sections. However, the orientation of the fibers at the high magnification breakpoint (Figure 42) still exhibits the same behavior as before, with the fibers orienting parallel to the strain direction. A similar phenomena is also seen both the low magnification (Figure 43) and high magnification (Figure 44) images of cellulose nitrate mats treated for 20 minutes in 1:9 (v:v) acetone to water. In both treatment cases, a slight change in the interaction of the fibers can be seen under low magnification, but this change is not strong enough to show a significant differences of the fibers zoomed in at the breakpoint.

Not surprisingly, the strongest treatment of 1:9 (v:v) acetone to water for 24 hours produced the most dramatic results. Although the outline of fibers is still visible in the low magnification images (Figure 45), the interactions between these fibers is drastically different. Sections in the top right of the top image show amorphous ribbons of the mat that have clearly fused together, and well as the formaton of "craters" or circular holes on the mats surface, a sign that this treatment option is beginning to reach the limit where some damage occurs. Upon examination of the high magnification images (Figure 46), the fibers are clearly not drawn in the direction of strain, as before, but broken as a cohesive piece.

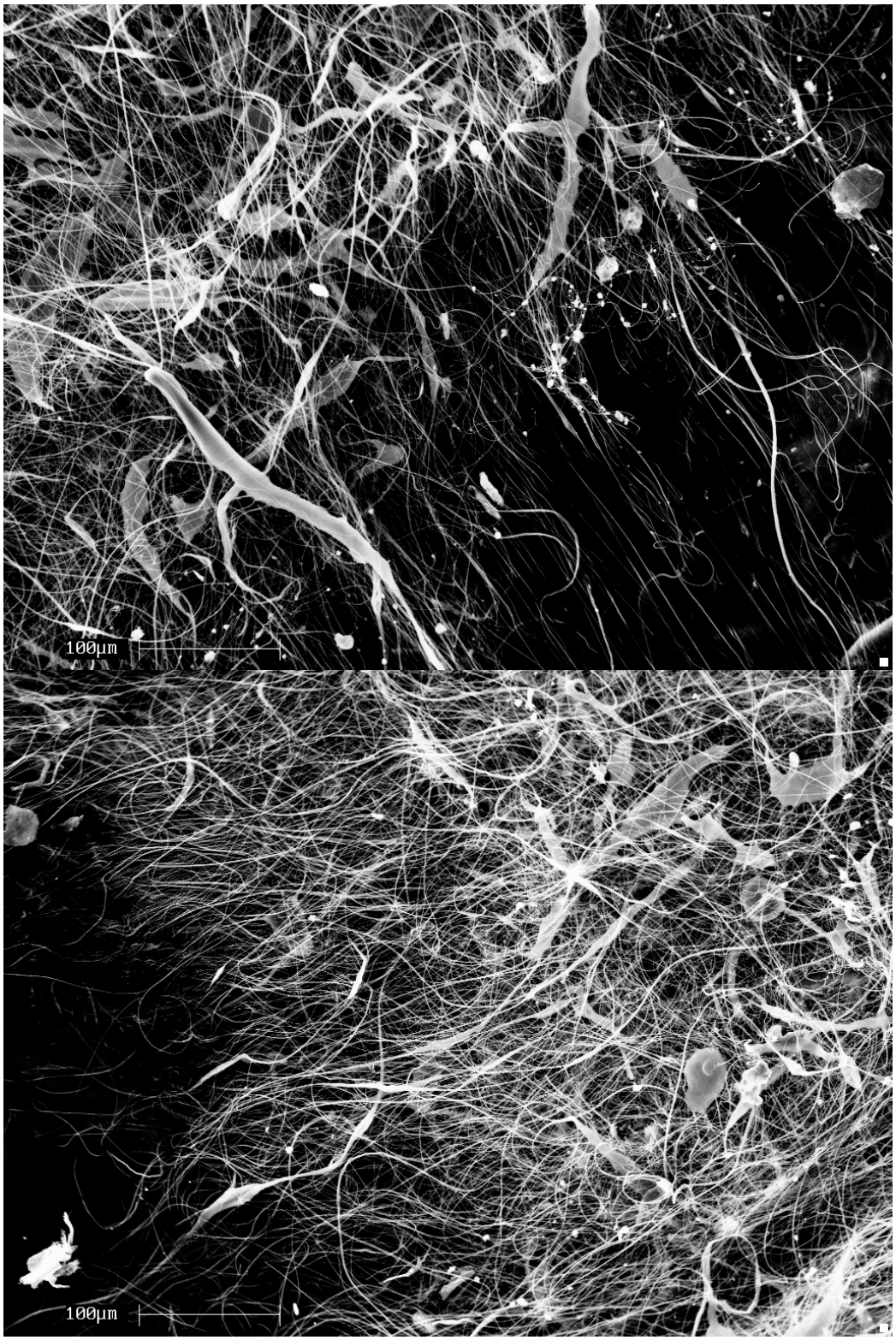

Figure 37: Low magnification SEM images of cellulose nitrate with no treatment with grain (above) and against grain (below).

Figure 38: High magnification SEM images of cellulose nitrate with no treatment with grain (above) and against grain (below).

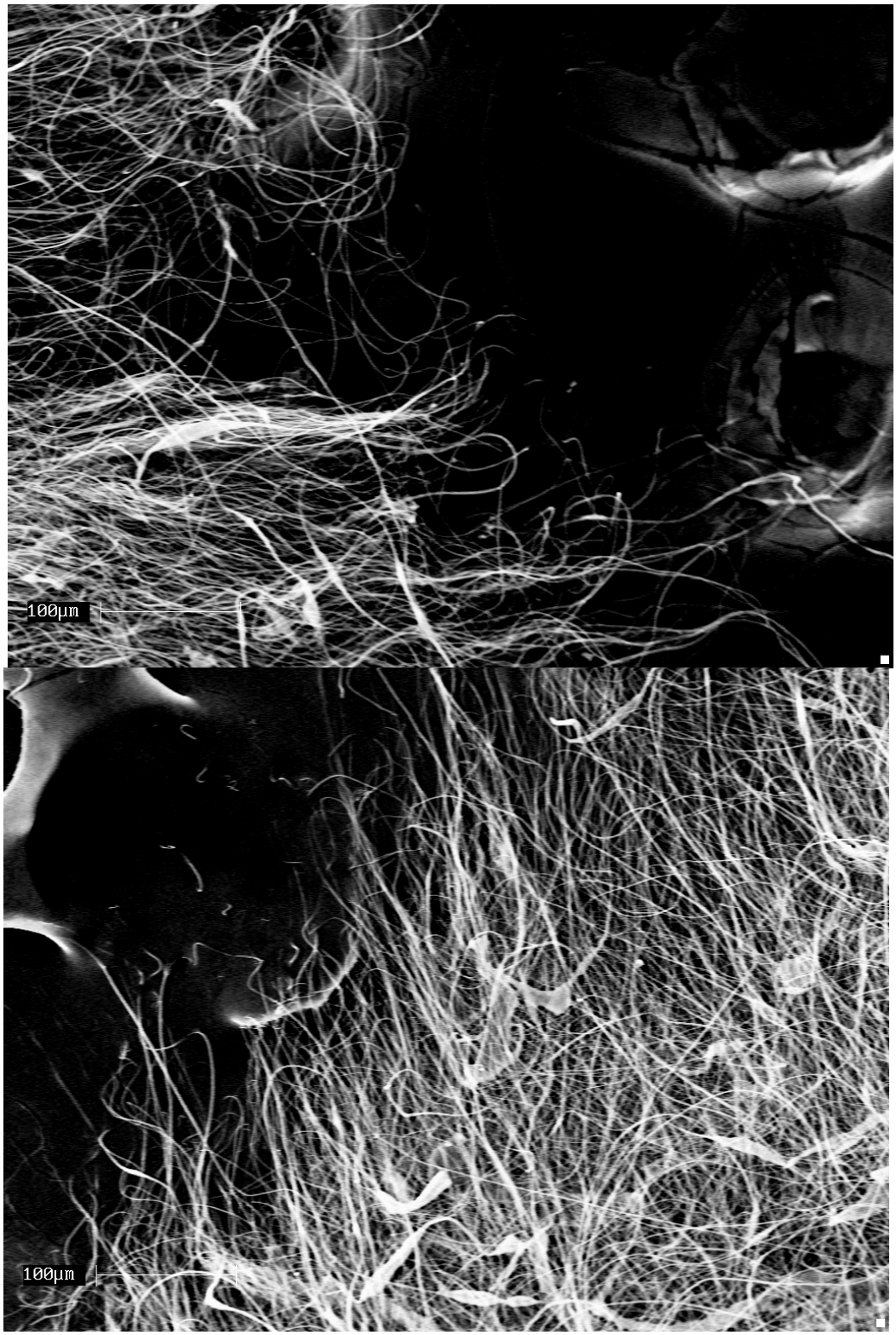

Figure 39: Low magnification SEM of cellulose nitrate after treatment with 1:19 (v:v) acetone:water for 20 minutes with grain (above) and against grain (below).

Figure 40: High magnification SEM of cellulose nitrate after treatment with 1:19 (v:v) acetone:water for 20 minutes with grain (above) and against grain (below).

Figure 41: Low magnification SEM of cellulose nitrate after treatment with 1:19 (v:v) acetone:water for 24 hours with grain (above) and against grain (below).

Figure 42: High magnification SEM of cellulose nitrate after treatment with 1:19 (v:v) acetone:water for 24 hours with grain (above) and against grain (below).

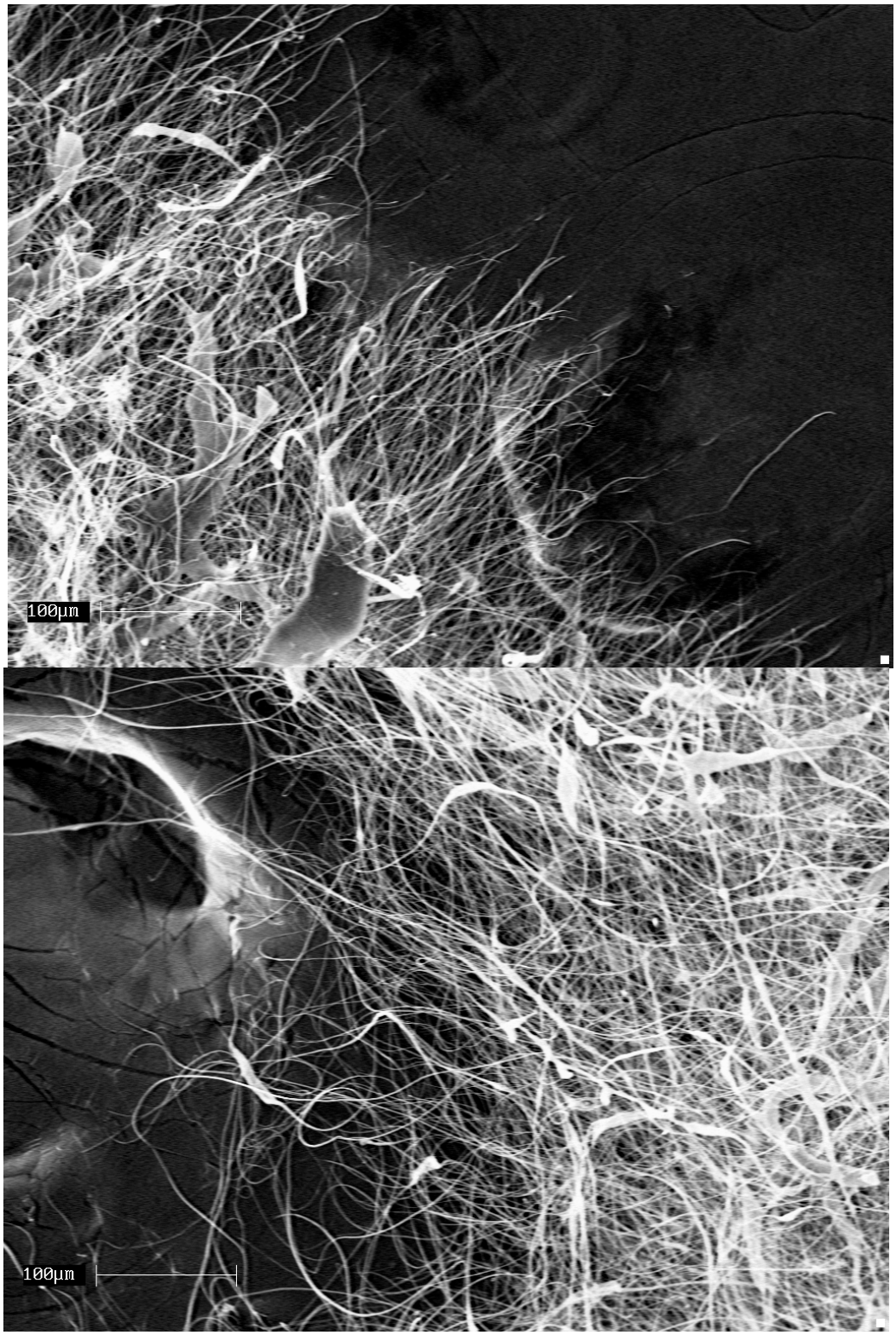

Figure 43: Low magnification SEM of cellulose nitrate after treatment with 1:9 (v:v) acetone:water for 20 minutes with grain (above) and against grain (below).

Figure 44: High magnification SEM of cellulose nitrate after treatment with 1:9 (v:v) acetone:water for 20 minutes with grain (above) and against grain (below).

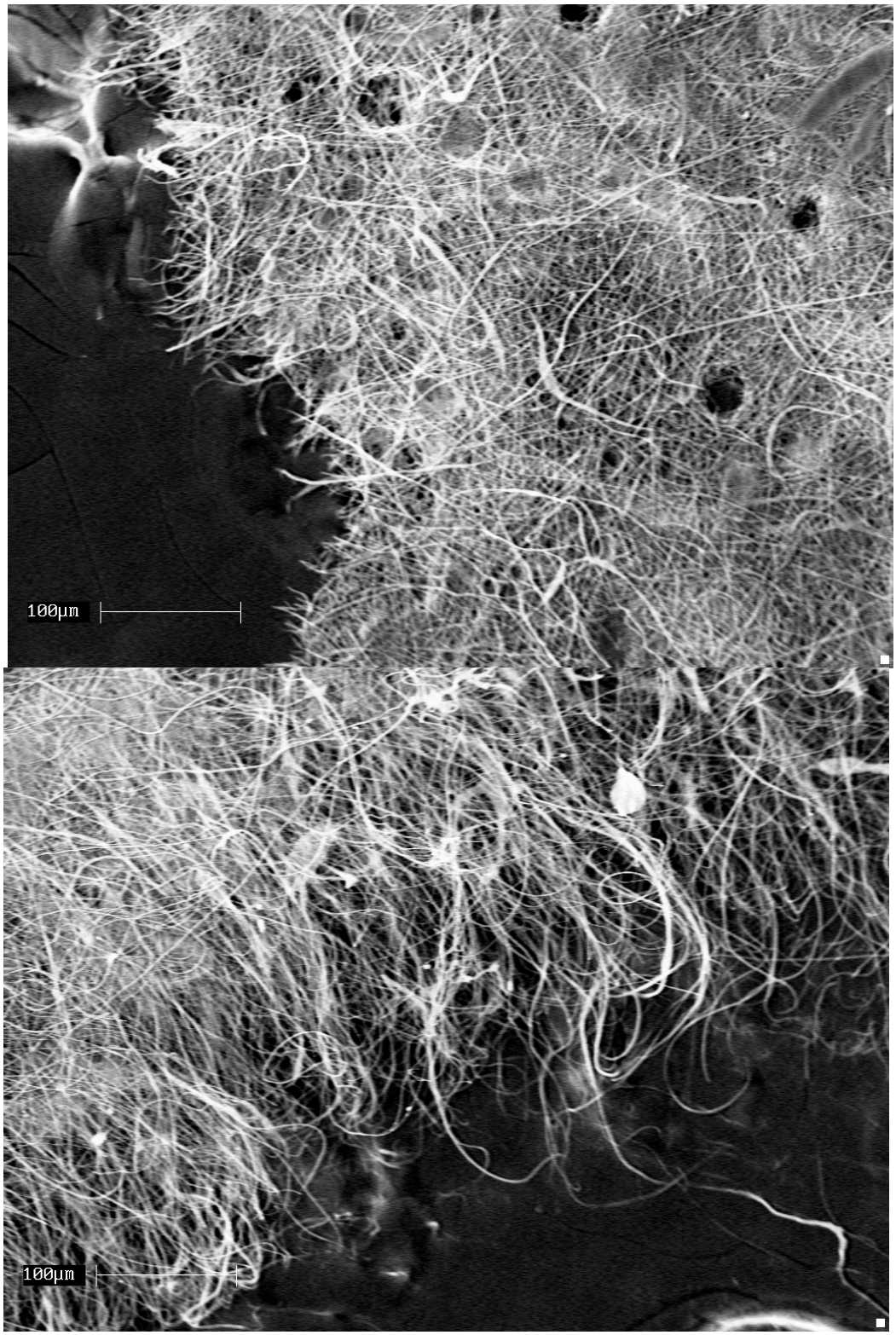

Figure 45: Low magnification SEM of cellulose nitrate after treatment with 1:9 (v:v) acetone:water for 24 hours with grain (above) and against grain (below).

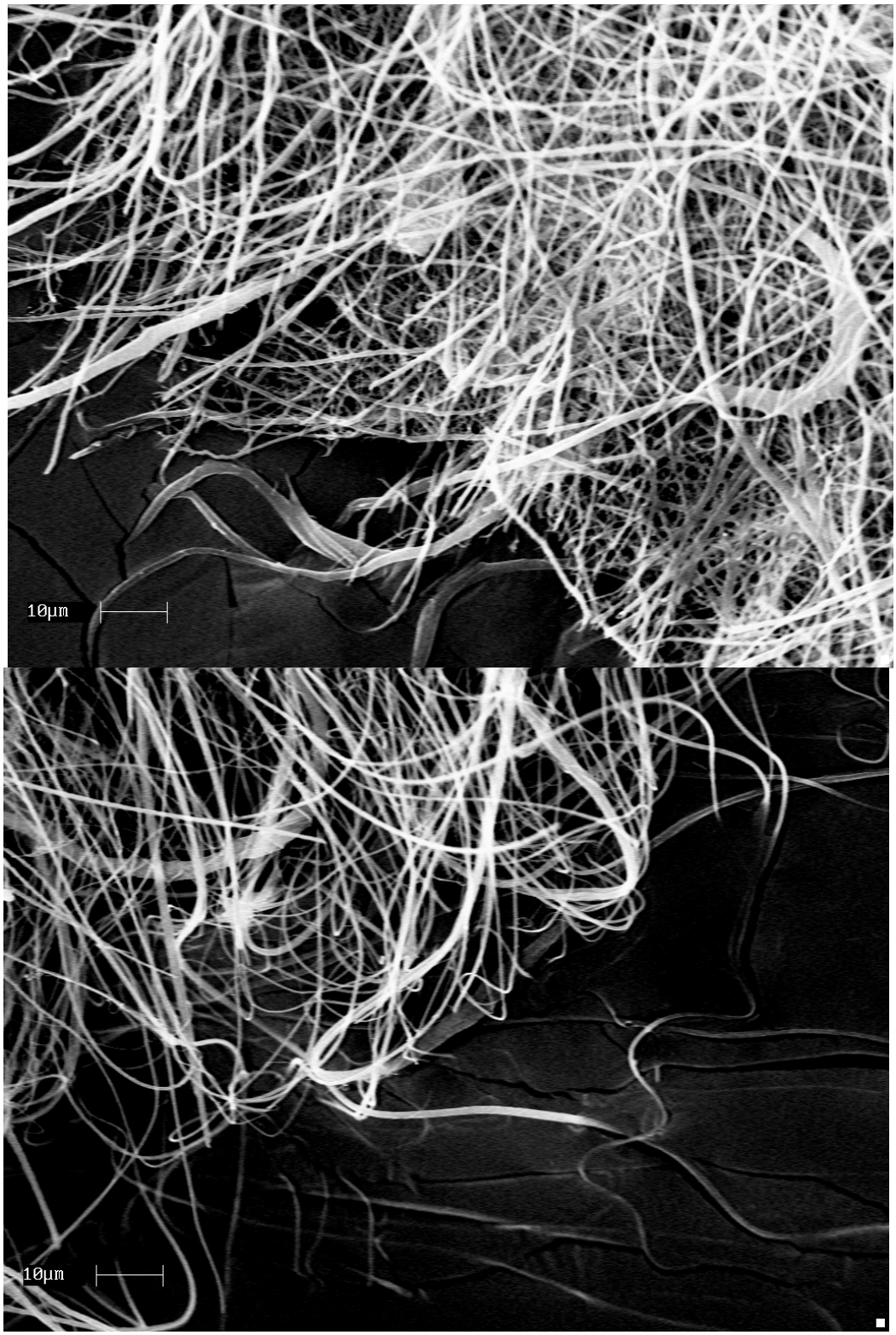

Figure 46: High magnification SEM of cellulose nitrate after treatment with 1:9 (v:v) acetone:water for 24 hours with grain (above) and against grain (below).

Pore Size Measurement

Cellulose Acetate

Just as with increased cohesion, cellulose acetate appears to show a significant decrease in pore size as treatments become longer and harsher (Figure 47). After even the mildest treatment, a significant decrease in average pore size can be seen when compared to the untreated sample cut with the spin grain. In addition, each sample cut against the spin grain appears to have a slightly smaller pore size than its counterpart cut with the spin grain but treated under the same conditions.

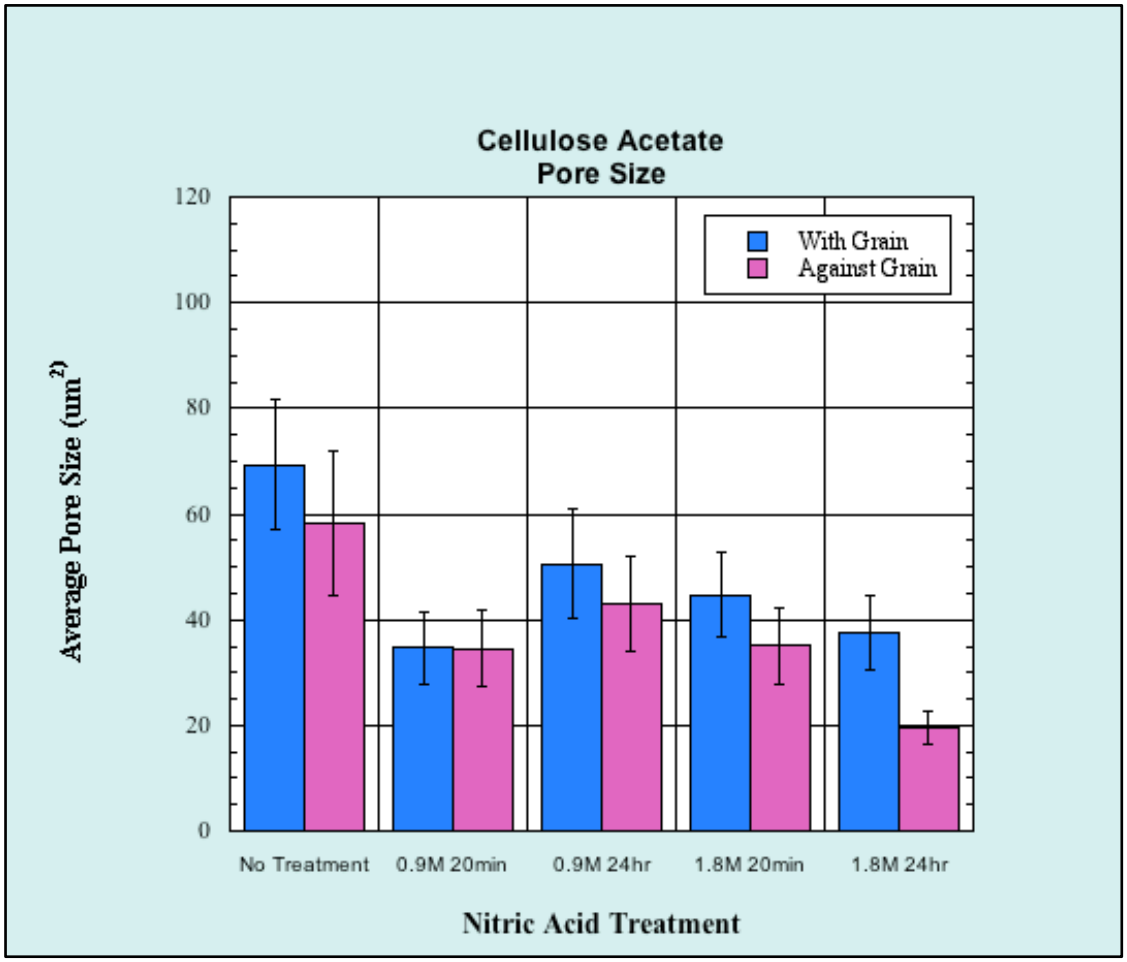

Figure 47: Average pore size of cellulose acetate mat after various nitric acid treatments.

Cellulose Nitrate

Unlike cellulose acetate, the samples made of cellulose nitrate do not seem to show a significant change in average pore size before and after treatments, with the exception of the harshest treated sample cut with the spin grain (Figure 48). In general, the average pore size was slightly above twenty square microns.

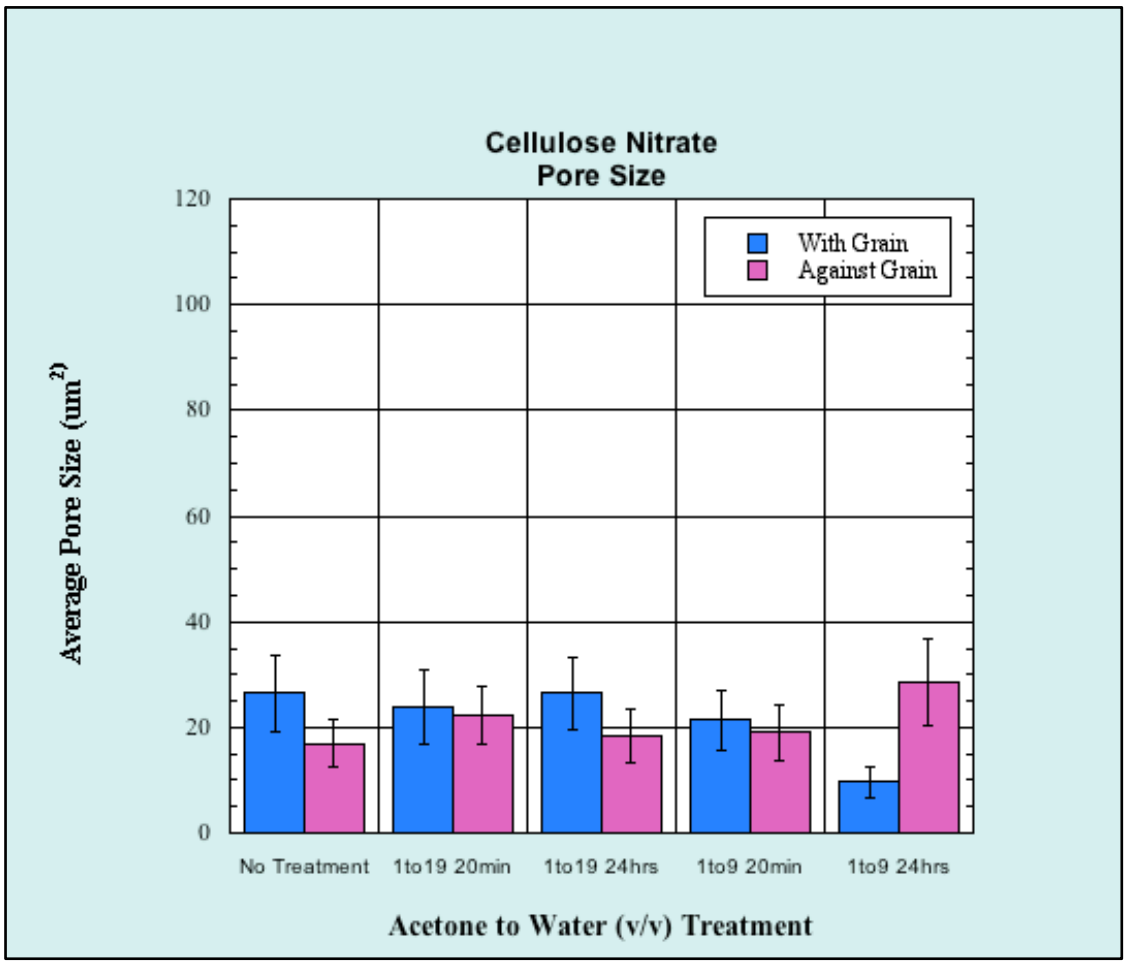

Figure 48: Average pore size of cellulose nitrate mat after various acetone treatments.

CHAPTER 4

Conclusions

Cellulose Acetate

Initially, it was hypothesized that (1) cellulose acetate could consistently be made into uniform solutions, (2) these cellulose acetate solutions could be electrospun into nanofibers, ultimately forming nonwoven mats, and that (3) the mechanical, chemical, and physical properties of these mats could be manipulated through controlled nitration. Through this project, these hypotheses were supported.

Cellulose acetate was consistently made into 17 wt% solutions by being dissolved in an 85:15 (v:v) acetone to water solvent system. These solutions were electrospun both on large and small scale to produce nonwoven fiber mats, which were ultimately subjected to various concentrations of nitric acid for various amounts of time as a finishing treatment. Changes in the mechanical, chemical, and physical properties of these mats were then observed.

Changes in the mechanical properties were measured through tensile tests. During all treatment options, the averaged tensile properties such as the young's modulus, extension to break, and force at break did not produce a large change (Figure 8 through Figure 10). This suggests that the treatments did not produce a large change in the overall morphology of the samples, and most importantly did not decrease the samples original strength or elasticity. In addition, these properties did not seem to overwhelmingly favor either direction in which the sample was cut (with or against the grain), suggesting that the material is isotropic in the case of its strength and elasticity. Upon examining the

stress vs strain curves, however, a change in the nature of the breaks was observed, causing the breaks to be sharp in all cases without treatment (Figure 11) to semi-sharp with the harshest treatment (Figure 15).

Changes in the chemical and physical properties of the cellulose acetate mats were observed through FTIR, XPS, and SEM, respectively. During FTIR, a large change in the heights of the peaks at 1738 and 1639 cm^{-1}, which correspond to acetate and nitrate groups respectively, could not be readily seen in the full FTIR spectra (Figure 24). Further analysis of these peaks suggested an increase in the nitration which would be consistent with nitration at the surface of the fiber only (Figure 25). However, upon elemental analysis of the surface using XPS, no nitrogen was present although a chemical reaction seemed to have occurred (Table 4). Upon examination of the SEM images, amorphous regions began to appear in the cellulose acetate mats after each treatment, with the most drastic of these being visible in the harshest treatment (Figure 27 to Figure 36). In addition, the pore size appeared to decrease after treatment (Figure 47). This suggests a slight change in the morphology of the fiber mats.

Cellulose Nitrate

Similar to cellulose acetate, it was hypothesized that (1) cellulose nitrate could consistently be made into uniform solutions, (2) these cellulose nitrate solutions could be electrospun into nanofibers, ultimately forming nonwoven mats, and that (3) the mechanical and physical properties of these mats could be manipulated through controlled nitration. Based on the data obtained, these hypotheses were supported.

Cellulose nitrate was consistently made into 12 wt% solutions by being dissolved in pure acetone. These solutions were electrospun both on large and small scale to produce nonwoven fiber mats, which were ultimately subjected to various concentrations of acetone in water for various amounts of time as a finishing treatment. Changes in the mechanical and physical properties of these mats were then observed.

Changes in the mechanical properties were measured through tensile tests. During all treatment options, the average extension to break, and force at break did not produce a statistically significant change (Figure 17, Figure 18). This suggests that the treatments did not produce a large change in the overall morphology of the samples, and most importantly did not decrease the samples original strength or elasticity. As with cellulose acetate, these properties did not seem to overwhelmingly favor either direction in which the sample was cut (with or against the grain), suggesting that the material is isotropic in the case of its strength and elasticity even after all treatments.

Intriguingly, however, a different result is present when examining the Young's modulus (Figure 16). For this property, there seems to be a statistically significant increase in the young's modulus between the no treatment option and the harshest treatment option when analyzing samples cut against the grain. This change is likely due to an increase of bonding between the surface of the fibers within the mat. This increased bonding works to maintain any anisotropic orientation, which may have been present during the spinning process, by preventing the fibers from being drawn parallel directly before breaking.

Upon examining the stress vs strain curves (Figure 19 through Figure 23), an increase in cohesiveness after treatment was also observed. As treatments

became longer and harsher, the shape of the curve evolved from pseudo-parabolic with gradual breakpoints in the plastic region (Figure 19a, samples 4 and 5) to almost linear with sharp breakpoints in the elastic region (Figure 23a, sample 2). This change is consistent with the change in the material from disconnected fibers to one, fully connected piece.

Observations of changes in the physical properties of the cellulose nitrate mats were also confirmed through SEM (Figure 37 through Figure 46). Analysis of the average pore size did not show a significant different in pore size before and after treatment (Figure 48). However, examination of both low and high magnification images at the breakpoints showed a stark change between the properties of the mats before and after treatment. In the images of the samples before treatment, the samples appeared to have drawn the fibers parallel to eachother before breaking (Figure 37, Figure 38). This suggests that the strength of the entanglement between the fibers was not as strong as the fibers themselves, causing them to reorient before breaking. In contrast, after treatment with 1:9 (v:v) acetone to water for 24 hours, the harshest treatment option, a completely different break behavior is observed (Figure 45, Figure 46). Rather than reorient, the fibers are strongly locked into a multi-fiber web. Therefore, rather than reorienting and breaking a fiber at a time like the untreated fibers, these treated fibers break sharply as one cohesive piece.

Overall

Ultimately, both approaches produced nanofiber mats. However, only cellulose nitrate ultimately had nitrate groups present at the fiber surface. Cellulose acetate and cellulose nitrate presented comparable tensile properties. Both materials exhibited results on the same order of magnitude for the Young's

modulus, extension at break, and force to break. The average values of the young's modulus for cellulose acetate ranged from between 1.2 to 3.4 MPa per percent strain (Figure 8) and for cellulose nitrate, between 2.8 and 4.9 MPa per percent strain (Figure 16). Similarly, the force to break was between 0.018 and 0.038 kg_{force} (Figure 10) and between 0.032 and 0.044 kg_{force} (Figure 18) for cellulose acetate and nitrate, respectively. These close ranges of values in all cases suggest that both materials would withstand similar stress conditions, and one would not be an overwhelmingly better choice based on its quantitative tensile properties.

Based on the shape of the stress vs strain curves, nature of the breaks and SEM images, however, cellulose acetate and the most harshly treated cellulose nitrate would have starkly different ideal applications than untreated or mildly treated cellulose nitrate. All cases of cellulose acetate (Figure 11 through Figure 15, Figure 27 through Figure 46) and the 24 hour treatment with 1:9 (v:v) acetone to water of cellulose nitrate (Figure 23, Figure 45, Figure 46) broke as one piece. This makes these materials ideal for applications where cohesion between fibers is necessary, such as within a microfluidic system where unanchored fibers could be washed away. Conversely, untreated and mildly treated cellulose nitrate membranes (Figure 19 through Figure 22, Figure 27 through Figure 44) did not break as a strongly cohesive piece, making these materials more ideally suited for applications where less cohesion is necessary. Testing these materials in these applications would be a valuable avenue for future work.

REFERENCES

[1] Thostenson, Erik T., Zhfeng Ren, and Tsu-Wei Chou. "Advances in the Science and Technology of Carbon Nanotubes and Their Composits: A Review." Composites Science and Technology 61 (2001): 1899-1912.

[2] Lee, Byoungho. "Review of the Present Status of Optical Fiber Sensors." Optical Fiber Technology 9.2 (Apr 2003): 57-79.

[3] Kumbar, S.G., R. James, S.P. Nukavarapu, and C.T. Laurenchin. "Electrospun Nanofiber Scaffolds: Engineering soft Tissues." Biomedical Materials 3 (2008): 1-15.

[4] Liang, Dehi, Benjamin S. Hsiao, and Benjamin Chu. "Functional Electrospun Nanofibrious Scaffolds for Biomedical Applications." Advanced Drug Delivery Reviews 59 (2007): 1392-1412.

[5] Barnes, Catherine P., Scott A Sell, Eugene D. Boland, David G. Simpson, and Gary L. Bowlin. "Nanofiber Technology: Designing the Next Generation of Tissue Engineering Scaffolds." Advanced Drug Delivery Reviews 59 (2007): 1413-1433.

[6] Ma, Zuwei, Masaya Kotaki, Ryuji Inai, and Seeram Ramakrashna. "Potential of Nanofiber Matric as Tissue-Engineering Scaffolds." Tissue Egnineering 11.1/2 (2005): 101-110.

[7] Lu, Ping, and Bin Ding. "Applications of Electrospun Fibers." Recent Patents on Nanotechnology 2.3 (2008): 169-82.

[8] Lukas, D., A. Sarkar, L. Martinova, K. Vosedalkova, D. Luasova, J. Chaloupek, P. Pokorny, P. Miles, J. Chvojka, and M. Komarek. "Physical Principles of Electrospinning (Electrospinning as a Nano-scale Technology of the Twenty-First Century)." Textile Progress 41.2 (2009): 59-140.

[9] Doshi, Jayesh, and Darrell H. Reneker. "Electrospinning Process and Applications of Electrospun Fibers." Journal of Electrostatics 35 (1995): 151-60.

[10] Li, Dan, and Younan Xia. "Electrospinning of Nanofibers: Reinventing the Wheel?" Advanced Materials 16.14 (2004): 1151-170.

[11] Weber, Patricia C., D.H. Ohlendorf, J.J. Wendoloski, and F.R. Salemme. "Structural Origins of High-Affinity Biotin Binding to Streptavidin." Science 243 (Jan 1989): 85-88.

[12] Orth, Reid N., T.G. Clark, and H.G. Craighead. "Avidin-Biotin Micropatterning Methods for Biosensor Applications." Biomedical Microdevices 5.1 (Mar 2003): 29-34.

[13] Polyak, Boris, Shimona Geresh, and Robert S. Marks. "Synthesis and Characterization of a Biotin-Alginate Conjugate and Its Application in a Biosensor Construction." Biomacromolecules 5 (2004): 389-96.

[14} Heeger, Peter S., and Alan J. Heeger. "Making Sense of Polymer-Based Biosensors." Proceedings of the National Academy of Sciences 96.22 (Oct 1999): 12219-21.

[15] Li, Lili, Margaret W. Frey, and Antje J. Baeumner. "Electrospun Polylactic Acid Nanofiber Membranes as Substrates for Biosensor Assemblies." Journal of Membrane Science 279.1-2 (2006): 354-63.

[16] Li, Lili, Margaret Frey, Dionysios Vynias, and Antje J. Baeumner. "Availability of Biotin Incorporated in Electrospun PLA Fibers for Streptavidin Binding." Polymer 48 (2007): 6340-347.

[17] Young, Robert J., and P. A. Lovell. Introduction to Polymers. London: Chapman & Hall, 1991.

[18] Mannhalter, Christine. "Biocompatibility of Artificial Surfaces Such as Cellulose and Related Materials." Sensors and Actuators B: Chemical 11 (1993): 273-79.

[19] Koropatkin, Nicole M., Himadri B. Pakrasi, and Thomas J. Smith. "Atomic Structure of a Nitrate-binding Protein Crucial for Photosynthetic Productivity. Proceedings of the National Academy of Science 103.26 (2006): 9820-825.

[20] Southern, E.M. "Detection of Specific Sequences Among DNA Fragments Separated by Gel Electrophoresis." Journal of Molecular Biology 98.3 (Nov 1975): 503-17.

[21] Van Oss, C. J., R. J. Good, and M. K. Chaudhury. "Mechanism of DNA (Southern) and Protein (Western) Blotting on Cellulose Nitrate and Other Membranes." Journal of Chromatograpy 391 (1987): 53-65.

[22] Frey, Margaret W. "Electrospinning Cellulose and Cellulose Derivatives." Journal of Macromolecular Science, Part C: Polymer Reviews 48.2 (2008): 378-91.

[23] Schiffman, Jessica D., and Caroline L. Schauer. "A Review: Electrospinning of Biopolymer Nanofibers and Their Applications." Polymer Reviews 48.2 (2008): 317-52.

[24] Li, Lili, and Margaret Frey. "Preparation and Characterization of Cellulose Nitrate-acetate Mixed Ester Fibers." Polymer 51.16 (July 2010): 3774-83.

[25] Kim, Kwangsok, Meiki Yu, Xinhua Zong, Jonathan Chiu, Dufei Fang, Yong-Soo Seo, Benjamin S. Hsiao, Benjamin Chu, and Michael Hadjiargyrou. "Control of Degradation Rate and Hydrophobicity in Electrospun Non-Woven Poly(D,L-Lactide Nanofiber Scaffolds for Biomedical Applications." Biomaterials 24 (2003): 4977-85.

[26] McKnight, Timothy E., Chorthip Peeraphatdit, Stephen W. Jones, Jason D. Fowlkes, Benjamin L. Fletcher, Kate L. Klein, Anatoli V. Melechko, Michael J. Doktycz, and Michael L. Simpson. "Site-Specific Biochemical Functionalization Along the Height of Vertically Aligned Carbon Nanofiber Arrays." Chemical Materials 18 (2006): 3203-11.

[27] Siro, Istvan, and David Plackett. " Microfibrillated Cellulose and New Nanocomposite Materials: A Review." Cellulose 17 (Feb 2010): 459-94.

[28] Tu, X., R.A. Young, F. Denes. "Improvement of Bonding Between Cellulose and Polypropylene by Plasma Treatment." Cellulose 1 (1994): 87-106.

[29] Kim, Dae-Young, Yoshiharu Nishiyama, and Shigenori Kuga. "Surface Acetylation of Baterial Cellulose." Cellulose 9 (2002): 361-7.

[30] Lu, J., and L. T Drzal. " Microfibrillated Cellulose/Cellulose Acetate Composites: Effect of Surface Treatment." Journal of Polymer Science Part B: Polymer Physics 48.2 (2009): 153-61.

[31] Urbanski, Tadeusz. Chemistry and Technology of Explosives. New York: Macmillan, 1964.

[32] Falconer, E. L., and C. B. Purves. "Assignment of Structure to Cellulose 3,6-Dinitrate." Journal of the American Chemical Society 79 (1957): 5308-10.

[33] DeNiro, Michael J. "The Effects of Different Methods of Preparing Cellulose Nitrate on the Determination of the D/H Ratios of Non-Exchangeable Hydrogen of Cellulose." Earth and Planetary Science Letters 54.2 (Jul 1981): 117-85.

[34] Rudd, J.H. "The Range of Radical Processes in Nitration by Nitric Acid." Chemical Society Review 20 (1991): 149-65.

[35] Pradhan, S., P. Bhattacharyya, and B.K. Chakrabarti. "Dynamic Critical Behavior of Failure and Plastic Deformation in the Random Fiber Bundle Model." Physical Review E: Statistical, Nonliner, and Soft Matter Physics 66.1.2 (Jul 2002): 1-13.

[36] Hidalgo, Raul Cruz, Ferenc Kun, and Hans J. Herrmann. "Bursts in a Fiber Bundle Model with Continuous Damage." Physical Review E: Statistical, Nonlinear, and Soft Matter Physics 64.6.2 (Dec 2001): 1-10.

[37 Kun, Ferenc, Stefano Zapperi, and Hans J. Herrmann. "Damage in Fiber Bundle Models." The European Physical Journal B: Condensed Matter and Complex Systems 17.2 (1999): 1-9.

[38] Fennessey, Sian F., Angelo Pedichini, and Richard J. Farris. "Chapter 21: Mechanical Behavior of Nonwoven Electrospun Fabrics and Yarns." Polymeric Nanofibers. American Chemical Society Symposium Series 918 (Feb 2006): 300-18.

[39] Gardner, Douglas J., Gloria S. Oporto, Ryan Mills, and My Ahmed Said Azizi Samir. "Adhesion and Surface Issues in Cellulose and Nanocellulose." Journal of Adhesion Science and Technology 22 (2008): 545-67.

[40] You, Young, Sung Won Lee, Seung Jin Lee, and Won Ho Park. "Thermal Interfiber Bonding of Electrospun Poly(L-Lactic Acid) Nanofibers." Materials Letters 60 (2006) 1331-3.

[41] Hendrick, Erin, Margaret Frey, Erik Herz and Ulrich Weisner. "Cellulose Acetate Fibers with Fluorescing Nanoparticles for Anti counterfeiting and pH-sensing Applications." Journal of Engineering Fibers and Fabrics 5.1(2010): 21-30.

[42] Moore, W. R., J. A. Epstein, A. M. Brown, and B. M. Tidswell. "Cellulose Derivative-Solvent Interaction." Journal of Polymer Science 23.103 (1957): 23-46.